WILLIAM LETTIS & ASSOCIATES, INC.

Final Technical Report

Holocene Slip Rate and Paleoearthquake History of the Green Valley Fault at Lopes Ranch Cordelia, California

Prepared for:

U.S.Geological Survey
National Earthquake Hazards Reduction Program
Award No. 03HQGR0094

Prepared by:

William Lettis & Associates, Inc.
1777 Botelho Drive, Suite 262
Walnut Creek, CA 94596

June 2004

FINAL TECHNICAL REPORT

HOLOCENE SLIP RATE AND PALEOEARTHQUAKE HISTORY OF THE GREEN VALLEY FAULT AT LOPES RANCH CREEK, CORDELIA, CALIFORNIA

Recipient:
[1]William Lettis & Associates, Inc.,
1777 Botelho Dr., Ste. 262, Walnut Creek, CA 94596
(925) 256-6070 phone; (925)256-6076 fax; URL www.lettis.com

[2]William Lettis & Associates, Inc.,
999 Andersen Dr., Ste.120, San Rafael, CA 94901
(415) 721-1320 phone; (415) 453-8519 fax

Principal Investigators:
John N. Baldwin[1], and Richard D. Koehler[2]
baldwin@lettis.com; koehler@lettis.com

Contributors:
Steve Thompson[1] and Ashley Streig[1]
thompson@lettis.com; streig@lettis.com

Keywords:
Research on paleoearthquake chronologies, slip-rates, and recurrence

Program Element II

U.S. Geological Survey
National Earthquake Hazards Reduction Program
Award Number 03-HQ-GR-0094

June 2004

Research supported by the U.S. Geological Survey (USGS), Department of the Interior, under USGS award number 03-HQ-GR-0094. The views and conclusions contained in this document are those of the authors and should not be interpreted as necessarily representing the official policies, either expressed or implied, of the U.S. Government.

Award 03-HQ-GE-0094

HOLOCENE SLIP RATE AND PALEOEARTHQUAKE HISTORY OF THE GREEN VALLEY FAULT AT LOPES RANCH CREEK, CORDELIA, CALIFORNIA

John N. Baldwin and Richard D. Koehler, III
William Lettis & Associates, Inc., 1777 Botelho Drive, Suite 262, Walnut Creek, CA 94596
phone: 925-256-6070, fax: 925-256-6076
baldwin@lettis.com; koehler@lettis.com

ABSTRACT

The Concord-Green Valley fault system (CGVF) is part of the eastern San Andreas fault system, and traverses the densely populated I-680 and I-80 corridor. The CGVF is composed of at least two major fault segments from south to north: Concord fault (16-to 24-km long) and Green Valley fault (29-to 43-km-long). The Green Valley fault is composed of a northern and southern segment that extend from the northern shores of Suisun Bay to Wooden Valley, east of Napa. Information on the paleoearthquake history and slip rate of the Green Valley fault are sparse; however, this investigation at the Lopes Ranch Creek site, 9 km south of Cordelia, provides initial long-term slip rate information for the southern Green Valley fault.

At the Lopes Ranch Creek site, an ephemeral creek preserves the cumulative dextral separation of an abandoned north-trending paleochannel located east of the main Green Valley fault. The initial slip rate yielded by the Lopes Ranch Creek site is close to the historical slip and creep rates for the Green Valley fault. Preliminary estimates of cumulative right-lateral displacement of a prominent paleochannel deposit range from 31 to 58 meters. Radiocarbon analyses of charcoal collected from a burn horizon directly above the offset channels provide a minimum age for the offset channel deposits of 14,080 to 15,380 cal yr B.P. Based on the estimated cumulative displacement and minimum age of the offsite paleochannel deposits, a preliminary long-term slip rate for the southern Green Valley fault is 2 to 4 mm/yr. Previous slip rate studies at Lopes Ranch provided an initial slip rate of 3.8 to 4.8 mm/yr (over the last 300 years), consistent in part with the long-term slip rate yielded by this study. These geologic slip rates also are close to the 14.7-year average creep rate of 4.4 ± 0.1 mm/yr for the southern Green Valley Fault. The slip rate of the southern Green Valley fault is similar to the geologic slip rate of the Concord fault (3.4 ± 0.3 mm/yr) which likely connects with the southern Green Valley fault across a narrow right stepover below Suisun Bay.

Because of: (1) the uncertainties on the location of the paleochannel deposit directly at the fault zone, and (2) the preliminary nature of the investigation at Lopes Ranch Creek, additional studies are necessary to refine the long-term slip rate for the fault. Furthermore, the fine-grained nature and massive composition of the deposits did not provide appropriate conditions for assessing event timing information. Therefore, this initial study provides information primarily on the long-term slip rate of the southern Green Valley fault.

TABLE OF CONTENTS

ABSTRACT i
1.0 Introduction 1
2.0 Regional Setting 3
2.1 Previous Investigations along the Southern Green Valley Fault 3
2.2 Geomorphology of the Lopes Ranch Creek site 4
3.0 Results 6
3.1 Near Surface Stratigraphy 6
3.1.1 Trenches T-1, T-2, and T-4 7
3.1.2 Trench T-3 9
3.2 Near Surface Structural Relations 9
3.3 Displaced Paleo-Lopes Creek Channel Deposits 12
3.4 Creep Rate Assessment 12
4.0 Discussion 14
4.1 Tectonic Model for Paleochannel Offset at Lopes Ranch Creek 14
4.2 Preliminary Slip Rate of the Green Valley Fault 15
4.3 Conclusions 15
5.0 References 17

LIST OF TABLES

Table 1. Radiocarbon Analyses: Trench T-1, Lopes Ranch Creek Site 6

LIST OF FIGURES

Figure 1. Concord-Green Valley fault system, and other faults in the eastern San Francisco Bay area.

Figure 2. Fault location map showing location of previous paleoseismic and geoarchaeological studies on the Green Valley fault (modified from Bryant, 1982; and Baldwin et al., 1998).

Figure 3. Aerial photograph interpretation of the Southern Green Valley fault at the Lopes Ranch Creek site showing Quaternary geologic map units and fault traces. Photograph from 1996.

Figure 4. Photograph looking southeast showing linear saddle and fault valley extending southeast of the Lopes Ranch Creek site. Mount Diablo and Suisun Bay are in the background.

Figure 5. Photograph looking northwest showing broad alluvial fan incised by Lopes Ranch Creek (trending across middle ground). Lopes Ranch Creek bends to the north at the Green Valley fault and follows a linear stream valley to the northwest.

Figure 6. Detailed topographic map of the Lopes Ranch Creek site. Green and purple lines through trenches T-1 and T-4 represent the western and eastern limit of buried channel deposits. Orange line represents the thalweg of the deepest channel deposit (unit 7A). The minimum and maximum displacements of unit 7A are also shown.

Figure 7. Log of trench T-1, south wall.

Figure 8. Log of trench T-2, south wall.

Figure 9. Log of trench T-4, south wall.

Figure 10. Log of trench T-3, south wall.

Figure 11. Photographs of Green Valley fault zone in trench T-1 showing altered sandstone bedrock. 11A shows altered sandstone bedrock in fault contact with darker brown alluvium; 11B shows older shear planes being replaced by calcium carbonate in sandstone bedrock.

Figure 12. Low-angle fault juxtaposing weathered bedrock on the west over Quaternary alluvial fan deposits on the east in the south wall of trench T-1. Photograph corresponds with Station 22m.

Figure 13. Photograph of south wall of trench T-4 showing paleochannel unit 7A overlain by thinner paleochannels in unit 9.

Figure 14. A) View to west shows rock wall crossing central fault strand of the Green Valley fault and showing displacement. B) Photograph looking east showing right-laterally deflected rock wall across Green Valley fault.

Figure 15. Two alternative models to explain the observed buried paleochannel deposits at Lopes Ranch Creek.

LIST OF APPENDICES

Appendix A - Lithologic and Pedologic Descriptions

1.0 INTRODUCTION

This report presents the findings of a preliminary paleoseismic investigation of the southern segment of the Green Valley fault at Lopes Ranch, southwest of Cordelia, in Solano County, California (Figure 1). At Lopes Ranch we have identified an ephemeral creek-Lopes Ranch Creek-that obliquely crosses the main active zone of the Green Valley fault (GVF), and is right-laterally displaced. The primary goal of the investigation at the Lopes Ranch Creek site is to provide initial information on the long-term geologic slip rate of the Green Valley fault, and evaluate the possibility to obtain information on the timing of past Holocene surface ruptures on the fault. Currently only sparse data on Holocene slip rate and earthquake timing are available for the Green Valley fault. Slip rate data are an essential input parameter for probabilistic earthquake hazard estimates for future earthquake occurrence in the San Francisco Bay region (WGCEP, 2003). The preliminary slip rate information developed in this study provides a better characterization of the GVF than currently exists and also may provide a better understanding of slip distribution along strike-slip faults in the eastern San Francisco Bay area between the Concord, Greenville, and other related structures in the vicinity.

Most of the dextral shear component of distributed Pacific-Sierra Nevada plate motion in the northern San Francisco Bay area is accommodated by three major right-lateral strike-slip faults or fault systems, including the San Andreas fault, Rodgers Creek-Healdsburg fault system, and Concord-Green Valley-Cordelia fault system (CGVF) (Figure 1). Plate motion is partitioned between these three major right-lateral strike-slip fault systems. The San Andreas fault has a slip rate of about 23 ± 2 mm/yr (Niemi and Hall, 1992; Prentice, 1989) and the Hayward-Rodgers Creek fault system has a slip rate of about 8 ± 2 mm/yr. (Lienkaemper and Borchardt, 1996; Schwartz and others, 1992). The remaining plate motion is distributed across the CGVF and other faults, although the rates and distribution of slip are poorly understood (Figure 1).

There are at least two end-member structural models that attempt to explain the origin of dextral slip on the CGVF system. These models differ significantly in the process of transferring slip between Bay Area strike-slip faults, and thus the models imply different earthquake hazards for the eastern San Francisco Bay region. One model (Ellsworth and others, 1982; Oppenheimer and Macgregor-Scott, 1992; WGNCEP, 1996) assumes that 4 to 7 mm/yr of slip from the northern Calaveras fault (Kelson and others, 1996; Simpson and others, 1999) is transferred eastward between Danville and Walnut Creek across a right stepover to the Concord fault. This model assumes that the presence of a series of left-lateral faults, which were the source of earthquake swarms in 1970 and 1990 (Oppenheimer and Macgregor-Scott, 1992), help transfer slip between the Calaveras and Concord faults, and that Walnut Creek is a pull-apart basin. This model implies much of the slip on the northern Calaveras fault (4 to 7 mm/yr) is transferred to the Concord fault. The second model (Unruh and Sawyer, 1997; Unruh and Lettis, 1999) hypothesizes that slip on the CGVF system is linked to slip on the Greenville fault to the southeast across a left-stepping restraining bend and the Mt. Diablo anticlinorium. Implications of this model are that: (1) slip on the CGVF is independent of the Calaveras fault, and thus slip on the northern Calaveras fault is transferred northwesterly across contractional structures within the East Bay Hills to the northern Hayward fault (Simpson and others, 1992; Unruh and Lettis, 1999); and (2) the slip rate on the CGVF may be less than earlier estimates, and may be closer to the poorly assessed slip rate of 2 ± 1 mm/yr recently estimated for the Greenville fault (Sawyer and Unruh, 2002). A third possibility is that slip is partitioned onto the CGVF system through a combination of both models, and that the GVF inherits slip from contractional structures mapped southeast and east of the GVF in the Sacramento-San Joaquin Delta including the Cordelia fault (Figure 1).

Current estimates of the geologic slip rate of the GVF are based on geologic data, aseismic creep rates and partly on the interpretation of slip transfer between either the northern Calaveras fault and Concord

fault, or the Greenville fault and the Concord fault. It is generally agreed that aseismic creep rates increase from south to north along the CGVF from about 4 mm/yr on the Concord fault to about 4.5 to 5 mm/yr on the GVF, near Cordelia (Galehouse, 1998; Galehouse and Lienkaemper, 2003) (Figure 1). Slip rates used in earlier regional strain-rate studies (8 ± 2 mm/yr; Kelson and others, 1992), probabilistic seismic hazard maps (6 ± 3 mm/yr; Petersen and others, 1996) and earthquake probability models (6 ± 2 mm/yr; WGNCEP, 1996; WGCEP, 1999; WGCEP, 2003) usually assumed that the slip rate on the CGVF exceeded the aseismic creep rate. Recent paleoseismic studies suggest a slip rate of 3.4 ± 0.3 mm/yr over the past 6,000 years at Galindo Creek along the Concord fault (Borchardt et al., 1999; Borchardt and Baldwin, 2001) and a minimum slip rate of 3.9 to 4.8 mm/yr over the past 310 years at Lopes Ranch along the GVF (Baldwin and Lienkaemper, 1999; Borchardt and Baldwin, 2001). Based on these recent studies the WGCEP (2003) estimate a slip rate of 5 ± 3 mm/yr for the GVF. Bryant (1982, 1991) and Unruh (1999 personal communication) estimate a long-term Quaternary slip rate of at least 3 mm/yr based on an unconstrained dextral separation (<20 km) of Pliocene Sonoma Volcanics.

Clearly, more information on the Holocene geologic slip rate of the GVF is necessary to improve our understanding of its earthquake potential and refine the structural models of the eastern San Francisco Bay region. Data developed in this study will better characterize the GVF, by providing constraints on the Holocene geologic slip rate. The study expands on our previous collaborative work with Mr. Jim Lienkaemper of the U.S. Geological Survey at Lopes Ranch, and provides refinement of slip rate estimates determined in that study (Baldwin and Lienkaemper, 1999).

2.0 REGIONAL SETTING

The Green Valley fault is an active, 29- to 43-km-long, dextral strike-slip fault that extends from north of Suisun Bay, near the northern termination of the Concord fault, to Wooden Valley in eastern Napa County (Figures 1 and 2). At Suisun Bay, the Concord fault steps right or bends about 5° to 10° more northerly, where it merges with the GVF beneath Suisun Bay (Figure 1). Geometrical differences along the GVF define a 14 ± 4-km-long northern segment and a 22 ± 3-km-long southern segment (WGCEP, 2003). The southern segment of the GVF extends northwest from Suisun Bay to near the Green Valley Golf Course (Figure 2). The northern GVF extends from near the Green Valley Golf Course to Wooden Valley (Figure 2). Along its entire length, the GVF is delineated by prominent tectonic geomorphology (e.g., right-laterally offset drainages, closed depressions, scarps, and tonal and vegetation lineaments) and is expressed as a complex anastomozing fault zone of at least two to three active fault strands. There also is an inferred down-to-the-east vertical component across the fault as suggested by stratigraphy, topography and trench exposures at Reservoir Lane and Lopes Ranch (Baldwin and Lienkaemper, 1999), as well as in numerous consultant trenches excavated along the southern segment of the GVF south of Interstate 80. Near Wooden Valley, the tectonic geomorphology abruptly terminates and the northward projection of the fault is less certain. Recent mapping and aerial reconnaissance (Baldwin et al., 1998) suggest that geologic slip is transferred, in part, to the northwest across a series of west-vergent folds and thrust faults that are part of the Atlas Peak-Foss Valley and Snow Flat-Lake Hennessey lineaments (Figure 1).

2.1 Previous Investigations along the Southern Green Valley Fault

Geologic slip rate and earthquake timing data are essential for evaluating the seismic potential of the southern GVF and for assessing its contribution to seismic hazards in the San Francisco Bay area. Despite the presence of prominent tectonic geomorphology, direct paleoseismic information on slip rate and timing of large-magnitude earthquakes along the southern GVF is limited to a recent study at Reservoir Road and Lopes Ranch (Baldwin and Lienkaemper, 1999) (Figures 2, 3, 4 and 5). Paleoseismic investigations in close proximity to the southern GVF have concentrated on the northern GVF at Wildhorse Ranch (Baldwin et al., 2002), and the Concord fault at Galindo Creek (Borchardt et al., 1999).

In a trench investigation at Reservoir Lane, about 4 km northwest of the Interstate 80 and Cordelia Junction, Baldwin and Lienkaemper (1999) excavated two trenches across the eastern active creeping strand of the GVF, which is expressed as a <0.5-m-high east-facing escarpment and vegetation lineament. Trench exposures showed that Bt and Bk soil horizons developed in fine-grained alluvial fan deposits were warped across the fault into an east-facing monocline. The vertical separation measured on this monocline diminishes to the north across the site from about 0.8 to 1 m in trench T-1 to about 0.4 m in trench T-2, from which Baldwin and Lienkaemper (1999) infer that the eastern and western traces merge into a single strand northwest of Reservoir Creek. Because of the lack of dateable materials and bedded stratigraphy at the site they were unable to evaluate the earthquake history of the fault. However, they were able to confirm that the style of deformation is characterized by down-to-the-east vertical separation across the creeping strand consistent with observations made in trenches at Freeborn Creek about 9 km southwest of Cordelia (Carey, 1991).

Approximately 0.4 km northwest of Lopes Ranch Creek (this study), Baldwin and Lienkaemper (1999), performed an initial paleoseismic study at Lopes Ranch that contributed valuable new data on the late Holocene behavior of the southern GVF including preliminary estimates of slip rate and earthquake timing. Baldwin and Lienkaemper (1999) used stratigraphic and structural relations in trench exposures as indirect evidence of coseismic surface-fault rupture. The relations included: (1) truncated units, (2) upward fault terminations, and (3) tilted and/or offset stratigraphic deposits. On the basis of trench

exposures, radiometric analysis of charcoal samples collected from faulted deposits, and re-interpretation of unpublished logs from trenches previously excavated at the site (Sims, 1993), they inferred that multiple surface-rupturing earthquakes have occurred on the GVF in the past 2,700 years and that the most recent earthquake (MRE) may have occurred between 310 and 220 cal yr B.P. (Figure 5; Baldwin and Lienkaemper, 1999). Additionally, a buried paleochannel deposit was estimated to be right-laterally offset 1.2 to 1.5 m across the fault, from which the authors inferred a poorly constrained minimum slip rate of 3.9 to 4.8 mm/yr over a 310-yr time period. Due to the short time period considered, this rate is significantly influenced by the timing of the most recent event and next future event. We note that Baldwin and Lienkaemper (1999) were unable to conclude unequivocally that the structural and stratigraphic relations observed in their trench and re-interpreted from previous trenches (Sims, 1993) were a result of coseismic surface-fault rupture and not a product of aseismic creep. Information from the initial study at the Lopes Ranch site must be considered preliminary until further studies are performed.

2.2 Geomorphology of the Lopes Ranch Creek site

As shown on Figure 1, the Lopes Ranch Creek site is located along the southern part of the southern GVF approximately 7.5 km northeast of Benicia, 8.5 km south of Cordelia, and about 0.4 km southeast of the Lopes Ranch paleoseismic site (Baldwin and Lienkaemper, 1999). The GVF in this area juxtaposes Jurassic, Cretaceous, and Tertiary sedimentary and metamorphic rocks of the Franciscan Complex and Great Valley Sequence on the west against Pliocene Sonoma Volcanics on the east (Fox, 1983; Crane, 1988; Wagner and Bortugno, 1982). Prominent geomorphic features expressed along the fault at the site include deflected stream channels, vegetation lineaments, linear drainages, east-facing scarps, springs and sags, and a broad linear saddle (wind gap) (Figures 3, 4, and 5).

Although most investigators interpret a single main fault trace at the Lopes Ranch Creek site, minor differences exist on its exact location. For instance, Frizzel and Brown (1976) show a single trace associated with a subtle east-facing scarp and an alignment of moist zones and vegetation contrasts northwest of the creek (shown as “east-facing scarp” on Figure 3). Sims (1993) interprets the main fault near or slightly west of the inferred abandoned Lopes Ranch Creek paleochannel (Figure 3). Bryant (1992) interprets a western trace associated with the east-facing scarp of Frizzel and Brown (1976) located directly northwest of the site and across Lopes Ranch Creek, and an eastern trace associated with a prominent photo-lineament and a linear sidehill bench developed within the Sonoma Volcanics directly east of the site (shown as “bedrock break in slope” on Figure 3). Bryant (1992), however, interprets the western trace as the main fault trace based on the presence of well-developed tectonic geomorphology and right-laterally deflected drainages crossing the fault. Our interpretation of aerial photography and site reconnaissance generally agrees well with the interpretations of these previous workers, with the exception that the linear feature present east of the site may be associated with landsliding, bedding, or compositional differences within the Sonoma Volcanics (Figure 3). We also map the main trace directly west of the inferred abandoned paleochannel of Lopes Ranch Creek similar to Sims (1993) based on the presence of a subtle northwest-trending, east-facing topographic escarpment and vegetation lineament developed in alluvial fan material (Figure 3). The main active trace of the Green Valley fault also is well expressed directly north of Lopes Ranch Creek by a subtle east-facing escarpment, alignment of springs and sags, and distinct vegetation lineament (i.e., Frizzel and Brown’s, 1976). Within the stream valley of Lopes Ranch Creek, the fault zone is broadly estimated from a widening of the creek valley and several near-vertical, caliche-coated fracture zones exposed in the creek banks. Based on geomorphology, the fault strikes about N25°W to N30°W and projects northwest toward our previous BAPEX Lopes Ranch trench site (Baldwin and Lienkaemper, 1999) (Figure 2). South of the Lopes Ranch Creek site, the Green Valley fault projects across a low drainage divide at the base of a steep southeast-facing slope and becomes obscured by numerous large complex landslides.

As shown on Figures 3, 5 and 6, the site geomorphology is characterized by a broad gently northeast-sloping alluvial fan that emanates from the steep slopes composed of Mesozoic sedimentary rocks located west of the site. The alluvial fan is deeply incised near its center by a prominent east-flowing unnamed creek (herein named Lopes Ranch Creek). The creek is relatively confined to a narrow channel west of the fault, and widens at the fault zone where it then becomes abruptly deflected to the north (Figure 6). Directly southeast of the deflection, or bend, is a late Holocene to modern (?) fluvial terrace located about 1 m above the present-day creek channel and nested against a topographically higher north-trending swale (Figure 3). On the basis of the swale's length, geometry and orientation (aligns with the present-day channel of Lopes Ranch Creek), we interpret the swale as an abandoned, partially filled paleo-stream valley. The inferred paleo-stream valley is located east of the interpreted main fault trace and appears to have been elongated or translated right-laterally along the fault zone approximately 50 m based on surface topography. The paleo-stream valley becomes progressively buried to the southeast by colluvial and alluvial deposits suggesting continual translation along the fault through time.

The Lopes Ranch Creek site was chosen for investigation because it has (1) excellent geomorphic relations that constrain the location of the main fault trace, (2) bedded late Holocene alluvial deposits including stream and alluvial fan deposits associated with Lopes Ranch Creek and colluvial deposits derived from the hillslope east of the site, (3) an apparent right-laterally separated paleo-stream valley near the crest of the present-day drainage divide, (4) minimal cultural disturbance, and (5) creek/fault intersection that is at a high angle making it a preferable slip rate site.

3.0 RESULTS

Our objectives at the Lopes Ranch Creek site were to characterize the long-term slip rate and evaluating the potential to obtain information on the timing of Holocene paleoearthquakes on the southern Green Valley Fault. Our approach was to expose near-surface stratigraphy across the GVF, and to identify and characterize the geologic evidence of several right-laterally offset buried paleochannel deposits. The scope of work included generating a detailed topographic map of the Lopes Ranch Creek site and excavation of four fault-normal trenches. Trenches T-1, T-2, and T-4 were excavated across a linear swale (inferred paleo-stream valley) southeast of the mouth of Lopes Ranch Creek, and trench T-3 was excavated across the fault on a broad alluvial fan northwest of the creek (Figures 3 and 6). Two radiocarbon samples were collected from a buried paleosol (unit 8) developed in fluvial overbank deposits. The radiocarbon analyses were performed by Beta Analytical, in Miami, by accelerator mass spectrometry. The results are presented in Table 1.

Table 1. Radiocarbon Analyses: Trench T-1, Lopes Ranch Creek Site

Sample Designation	Measured Radiocarbon Age (1-sigma) 14_C yr B.P.	13C/12C Ratio	Conventional Radiocarbon Age (1-sigma) 14_C yr B.P.	Calibrated Radiocarbon Age Range (2-sigma) cal yr B.P.	Probability Distribution (95%) Probability of Calibrated Age Interval	Interpreted Calibrated Radiocarbon Age (2-sigma) yr B.P.
LR-TIS-RC-7 (Beta-192079)	11980 ± 40	-25.8 0/00	11970 ± 40	13650-13770 13800-14150 14170-14300 14720-15210	(0.057) (0.725) (0.056) (0.162)	13,800 to 15,210
LR-TIS-RC-9 (Beta-192080)	12240 ± 40	-24.7 0/00	12240 ± 40	13850-13920 14080-14390 14590-15380	(0.031) (0.507) (0.462)	14,080 to 15,380

Note: Shaded results were used to estimate the age of the charcoal sample.

The results of this investigation include: (1) detailed descriptions of near surface stratigraphy and structure that provide information on the depositional history and tectonic evolution of the site; and (2) descriptions of paleochannel offsets that provide preliminary information on fault slip rate. We use these data to estimate a preliminary slip rate for the southern Green Valley Fault.

3.1 Near Surface Stratigraphy

The four trenches (T-1 to T-4) at the Lopes Ranch Creek site (Figure 6) exposed a sequence of latest Pleistocene to historic deposits overlying weathered sandstone and siltstone bedrock of the Upper Cretaceous to Upper Jurassic Great Valley Sequence (Figures 7, 8, 9 and 10). In general, the bedrock northeast of the fault scarp is overlain by: (1) a northeast-dipping distal alluvial fan deposit; (2) five massively bedded, relatively flat lying fluvial deposits that fill the paleochannel or swale of Lopes Ranch Creek; (3) two distal alluvial fan deposits that have a slight northeast dip where they have been warped over the scarp, but flatten towards the center of the swale; and (4) three late Holocene distal alluvial fan/colluvial deposits overlain by a historic deposit. For ease of description, we herein refer to these surficial deposits as the lower alluvium, middle fluvial sequence, middle alluvium, and upper alluvium,

respectively (units 2 through 15, Figures 7, 8, 9, and 10). In addition, trenches T-1 and T-4 exposed a sequence of nested paleochannels within the middle fluvial sequence (units 7A and 9A, Figures 7 and 9). The lithologic characteristics of these deposits are summarized in the following text, and are provided in more detail in Appendix A. We first describe stratigraphic relations in trenches T-1, T-2, and T-4 because these trenches are located next to each other southeast of the mouth of Lopes Ranch Creek. We then describe stratigraphic relations in trench T-3 northwest of Lopes ranch Creek. Finally, we attempt to correlate stratigraphic units between the two locations.

3.1.1 Trenches T-1, T-2, and T-4

Trench T-1 exposed bedrock southwest of the Green Valley fault (unit 1, Figure 7) consisting of fractured fine-grained sandstone and siltstone within the Upper Cretaceous to Upper Jurassic Great Valley Sequence (Wagner and Bortugno, 1982). The rock varies in color from tan to yellowish orange brown, and contains stringers of carbonate nodules oriented along subvertical fractures. A well developed anastomosing, dendritic fracture pattern occurs in the rock at the eastern end of the fault zone that may be related to hydrothermal alteration of the rock by fluids migrating through porous sandstone (Figure 11). Some sandstone clasts within siltstone at the western edge of the fault zone have been replaced with carbonate.

A possible ancient paleochannel deposit is present in the west-central part of trench T-1. Between stations 23 and 28 m, there is a zone of slightly darker massive fine sand and silt that has large carbonate nodules (shown as unit 1A on Figure 7). Based on a “u-shaped” channel morphology, where this zone is in contact with more resistant bedrock, it is possible that the zone represents a late Quaternary alluvial channel fill. This is supported by apparent gravel lag near the base of the deposit and an overall fining upward sequence. A similar feature is visible on the opposite trench wall showing a possible paleoflow direction subparallel to the fault zone. Alternatively, this zone could be a less resistant bedrock lithology that has been severely altered by soil development processes.

The stratigraphically oldest sediments northeast of the fault and presumably overlying bedrock is the lower alluvium (units 3 and 4). The lower alluvium is only exposed at the base of trench T-2 and consists of a slightly northeast dipping, massive, dark brown silt with trace sand (unit 3) that has weak soil development (unit 4) noted by a slightly darker color (Figure 8). Based on the northeast dip of these deposits, we infer that the lower alluvium represents a distal alluvial fan deposit that may have been transported south by slip on the Green Valley fault. The dip of unit 4 exceeds the bedding attitude of the overlying deposits and indicates that a paleo-Lopes Ranch Creek may have existed farther to the east than the present-day creek.

The middle fluvial sequence, which includes units 5, 6, 7, 7A, 8, 9, 9A, and 9B, is exposed northeast of the fault in trenches T-1, T-2 and T-4, and overlies an angular unconformity with the lower alluvium (unit 4). Unit 5 is a fluvial deposit that onlaps unit 4, consisting of massive, olive brown silt with approximately 15% red and tan mudstone and sandstone gravel clasts that occur in discontinuous pockets and lenses. Unit 6, an olive brown clay with trace subrounded mudstone and sandstone gravel clasts and two discontinuous channel deposits, overlies unit 5 and represents fluvial overbank deposition within the Lopes Ranch Creek stream valley. In trench T-2 there is a subtle buried, poorly developed pedogenic soil development in unit 6. Unit 6 grades upward into unit 7, which is characterized by an olive brown clayey silt with weak bedding and gravel stringers. Within unit 7, unit 7A is a distinct, prominent channel thalweg deposit incised into unit 6, and that is present in trenches T-1 and T-4. Unit 7-A consists of a sandy silt matrix with pockets of grain supported subrounded to subangular sandstone and siltstone gravels. Orientations along the base and margins of the channel and thalweg measured across the trench indicate a paleo-flow direction of N16ºE to N5ºE, similar to present-day Lopes Ranch Creek east of the fault zone.

A dark yellowish brown soil (unit 8) consisting of very fine carbonate nodules and weak clay films is developed into the top of unit 7 along the margin of the buried channel (Figures 7 and 8). A charcoal sample (LR-T1S-RC-9) collected from a burn horizon in trench T-1 near station 9 m and within unit 8, yielded a calibrated age of 13,850 to 15,380 yr B.P. (Figure 7 and Table 1). We use the age range of 14, 080 to 15,380 yr B.P. for the age of unit 8. This age range represents 97% of the 2-sigma calibrated age probability distribution for sample LR-TIS-RC-9 (Table 1). Detrital charcoal (LR-T1S-RC-7) sampled from the same unit, but near station 5 m and not within an apparent burn horizon yielded a calibrated age of 13,800 to 15,120 yr B.P. (Table 1). Because sample LR-T1S-RC-9 was collected from within a burn horizon, we infer that it formed in situ and thus represents a close minimum age (14,080 to 15,380 yr B.P) for the base of the deposit. The pre-Holocene age of unit 8 is consistent with the well developed soil profile developed throughout the eastern end of trench T-1 within units 10 to 12, which contains large carbonate nodules and filaments, prominent clay films, and pedogenic structure (see Appendix A for descriptions). Units 10 to 12 are located stratigraphically above unit 8, and thus, are younger in age. The pedogenic structure of the soil is consistent with other Bay Area soils formed during the early Holocene (10-7 ka) (Glenn Borchardt, 2003 personal communication).

Units 9 and 9A present in trenches T-1 and T-4, consist of massive clayey silt overbank deposits interbedded with sandy silt and gravel channel lenses (Figures 7 and 9). These deposits represent continued fluvial aggradation in the Lopes Ranch Creek stream valley likely in response to shallowing of the channel gradient and lengthening of the channel caused by fault creep and/or surface fault rupture on the Green Valley fault. In trench T-1, these fluvial deposits onlap and bury unit 8 east of station 10 m. Orientations of the unit 9A channels across the trench range from N10ºW to N27ºW and the channel plunges north between 0 and 3 degrees.

A faintly laminated, and weakly developed buried soil, consisting of olive brown clayey silt and trace sandstone and volcanic gravel (unit 9B) is developed locally in units 9 and 9A (trench T-4; Figure 9). This soil shows less soil development than Unit 8. Unit 9B is the uppermost unit of the middle fluvial sequence and represents the cessation of fluvial deposition in the paleo Lopes Ranch Creek channel. We infer that Lopes Ranch Creek abandoned its channel shortly after deposition of unit 9, allowing colluvial volcanic clasts derived from the Sonoma volcanics that underlie the slope east of the site to be incorporated into the soil.

The middle alluvium, which includes units 10, and 11, overlies the middle fluvial sequence (trenches T-1, T-2, T-4 and Figures 7 and 9). These deposits are generally uniform throughout the site, consisting of an olive brown sandy to silty clay with occasional discontinuous gravel lenses and trace fine carbonate nodules (unit 10), and a dark grayish brown silty clay with coarse angular blocky soil peds and trace fine carbonate nodules (unit 11). These deposits have gradational and wavy basal contacts and contain approximately 5-15% subangular to subrounded gravels composed of both sandstone and siltstone derived from the west and Sonoma volcanics derived from the east. Based on the clast lithologies sourced from the east and west and the lack of fluvial channel deposits, we infer that the middle alluvium post-dates the abandonment of the paleo Lopes Ranch Creek and represents the filling of the paleo Lopes Ranch Creek channel by alluvial fan sedimentation from the west and colluvial sedimentation from the east. Based on soil profile development, medium to thick clay films, coarse firm to very firm angular blocky ped structure, and fine secondary carbonate nodules (stage II development), we estimate an early Holocene age of the buried soil developed in units 10 (2Btk horizon) and 11 (2Bt horizon) (G. Borchardt, 2003, personal communication). This is consistent with the results of the radiocarbon analyses of the lower units indicating a very late Pleistocene age. Because units 10 and 11 bury units 8 and 9, we infer that the early Holocene likely represents a maximum limiting age for abandonment of paleo Lopes Ranch Creek.

The upper alluvium stratigraphically overlies the middle alluvium, and includes units 12, 12A, 13, 14, and 15 (trenches T-1, T-2, T-4; Figures 7 to 9). With the exception of units 12 and 15, these units maintain a constant thickness throughout the site. Unit 12 consists of a very dark grayish brown sandy silt to clayey silt that contains approximately 15% gravel (unit 12). Units 13 and 14 are two dark gray silt deposits that contain approximately 5% gravel. Unit 15, which contains horseshoes and nails, represents a small historical swale eroded by cattle that has been filled with silt reworked from units 13 and 14. The modern soil profile has developed through the upper alluvium and is characterized by an A- horizon with fine subangular blocky ped structure and no clay films (unit 14), an AB-horizon with medium subangular blocky ped structure and weak clay films (unit 13), and a BC-horizon parent material (unit 12) in trench T-1. Unit 12 dips slightly to the northeast from the bedrock high at the fault scarp near station 20 m. This unit represents a distal alluvial fan deposit, similar to the middle alluvium. We group it with the upper alluvium, however, based on the lack of soil development. Unit 12 may have been stripped partially by vertical displacement across the fault zone and planation from unit 13. The basal contact of unit 13 mimics the surface topography (flatter than unit 12). Modern alluvial/colluvial processes appear to have stripped units 11 and 12 (Figures 7, 8, and 9). Units 13 and 14 represent the latest stage of colluvial deposition in the paleo Lopes Ranch Creek stream valley.

3.1.2 Trench T-3

Similar to trench T-1, trench T-3 exposed bedrock southwest of the Green Valley fault (unit 1, Figure 10) consisting of fractured sandstone and siltstone within the Upper Cretaceous/Upper Jurassic Great Valley Sequence (Wagner and Bortugno, 1982). Southwest of the fault, bedrock is overlain by a distal alluvial fan deposits–units 2 and 3–which consists of a brown to dark yellowish brown clayey silt with well developed prismatic to columnar soil peds and prominent 3-5 cm long carbonate nodules. The basal part of this deposit (unit 2) contains clasts of bedrock, and represents the weathered top of bedrock mixed with alluvial fan materials. Northeast of the fault zone, units 1, 2, and 3 are in fault contact with unit 4 across a 0.25- to 1-m-wide fault gouge zone. Unit 4 consists of a dark brown clay to clayey silt with carbonate nodules and may correlate with unit 3 southwest of the fault. Units 5, 6, 7, and 8 overlie units 4 and 3, and may correlate with units 11, 12, 13, and 14 from trenches T-1, T-2, and T-4 southeast of the creek, respectively. Unit 5, which consists of a dark brown clayey silt to silty clay with coarse prismatic soil ped structure, is overlain by unit 6, a dark brown clayey silt with approximately 25% gravel. Stratigraphically above unit 6 is a weakly developed A-AB horizon soil profile, consisting of very dark gray silt with trace fine gravel (units 7 and 8). All of these deposits are interpreted to be distal alluvial fan deposits sourced from Lopes Ranch Creek, and appear to be locally thickened and folded across the fault.

3.2 Near Surface Structural Relations

The location of the southern Green Valley fault zone is constrained at the Lopes Ranch Creek site on the basis of exposures in two fault-normal trenches (T-1 and T-3) and prominent tectonic geomorphology, including a distinct vegetation lineament and east-facing scarp aligned with faults exposed in the trenches (Figures 3, 7, and 10). The trenches exposed an active eastern fault strand, a possible active western strand, and a zone of inactive bedrock faults between the two fault strands. These exposures show that the main active strand of the fault is located along the eastern side of the fault zone and coincides with the surface vegetation lineament and scarp crossed by trenches T-1 and T-3. Extensive shearing of Great Valley Sequence bedrock within the fault zone often is associated with calcium carbonate deposits along complex anastamosing fracture planes (Figure 11).

In trench T-1, striae preserved on a west-dipping low-angle fault surface between stations 18 and 21 m indicate a component of dip-slip displacement (Figure 7). In trench T-3, a similar low-angle, west-dipping fault contains fault striae that indicate oblique slip displacement with components of reverse and dextral slip. We observed no other reliable indicators of slip direction in the trench exposures (i.e. slickensides),

although it can be assumed based on historical observations of fault creep (Galehouse, 1998), site geomorphology, and trench exposures that the fault is dominated by right-lateral offset with a component of southwest-up vertical separation. Southwest-side up vertical separation is consistent with the presence of a bedrock topographic-high on the western side of the fault, as well as with observations at our trench exposures at Lopes Ranch and Reservoir Road, north of the site (Baldwin and Lienkaemper, 1999).

In trench T-1, the fault zone is at least 12-m-wide and includes multiple subvertical fractures and faults that strike from N18ºW to N50ºW with nearly vertical dips (Figure 7). The main active trace of the fault occurs along the eastern side of the zone and is defined by a 2.5-m-wide shear zone bounded on the east by a N30ºW-striking vertical fault associated with a 1 cm wide clay gouge and on the west by a low-angle fault dipping 26º southwest (Figure 12). A highly sheared alluvial fan deposit with abundant carbonate (unit 2) is incorporated into the fault between these two fault strands (Figures 7 and Figure 12). The low-angle fault projects up section into a 0.75-m-wide zone consisting of several west dipping fault strands or distinct fractures that extend upward from the main fault trace to the ground surface. The stratigraphy, including the modern soil, appears to be slightly warped down to the east across the west-dipping faults. The upper most low-to high-angle shears truncate units 8, 10 and 11, however, the upward projection of the shearing becomes diffuse in the overlying deposits, and faulting is based on prominent fracturing, and the presence of a shear fabric.

The lower gently dipping fault offsets unit 1b against unit 6, although it is difficult to observe significant offset across unit 8. This lower-most gentle dipping fault truncates a near-vertical fault that juxtaposes fluvial overbank deposits on the east (unit 6) against highly sheared alluvium on the west (unit 2). The only possible source for the fluvial overbank deposits is Lopes Ranch Creek, from which we infer that the fluvial deposits have been offset right laterally. The middle gently dipping fault clearly offsets units 8, 10 and 11 on the north wall of the trench although these relations are less clear on the south wall of trench T-1 (Figure 7). Distal alluvial fan deposits drape the eastern limit of the fault zone, but are not present west of the main trace (Figure 7). We infer that up-to-the-west vertical separation across the fault zone contributed to erosion and stripping of material west of the fault zone and subsequent deposition of colluvium east of the fault zone. This is consistent with striae observed along fault surfaces of the eastern strand that indicate dip-slip displacement. On the basis of the fault geometry, kinematic geometry, and displacement of stratigraphic deposits exposed in trench T-1, we interpret the complex faulting as accommodating transpressive deformation with the primary component of shearing being right-lateral strike-slip displacement, with a minor amount of reverse displacement. Also, based on the amount of displacement observed across many of the older units (below unit 8), as well as the prominent near-surface fracturing, we interpret the eastern fault strand as the main, active creeping strand of the Green Valley fault.

The stratigraphy in trench T-1 provides direct evidence of progressive vertical deformation over time. We infer that the steeper dips of units 8 and 10 than overlying units 11 and 12 is due to progressive rotation caused by down-to-the east movement across the fault zone. Because most of the older units are truncated at the fault and cannot be traced west, the amount of apparent vertical separation is unknown. We estimate minimum vertical separation by projecting the base of unit 8 toward the fault zone and assuming that the unit formerly overlay bedrock west of the fault, and has been removed by erosion with continual vertical displacement across the fault. The minimum vertical displacement under these assumptions is 0.8 m.

The western-most fault strand exposed in trench T-1 may be Holocene active (Figure 7). This fault strikes N18ºW, dips vertically and is characterized by calcium carbonate stringers along the fault plane. Fractures associated with the fault plane can be traced upward to within the overlying weathered bedrock profile, but not readily into the overlying Holocene alluvium (unit 13) unconformably overlying the bedrock. The fault juxtaposes fine-grained sandstone on the east against highly weathered sandstone or

Quaternary alluvium on the west. Although the fault cannot be traced vertically beyond the bedrock regolith, the overlying unit 13 thickens to the west across the fault zone. If the thickening is related to down-to-the west separation, this strand likely is middle to late Holocene active. No prominent shearing or fracturing is visible in the overlying massive Holocene colluvial and alluvial deposits similar to the other bedrock faults located to the east. The stratigraphic and structural relations encountered across the western fault strand suggest a low level of recent activity, if at all, compared to the main active eastern strand characterized by extensive fracturing, shearing, and truncation and warping of deposits.

In trench T-3, the fault zone is at least 8 m wide, and consists of three elements: 1) creep-related fractures, 2) a main fault trace, and 3) a low-angle west-dipping fault (Figure 10). The main active fault strand is exposed in trench T-3, defined by an approximately 0.75- to 0.25-m-wide gouge zone at the base of the trench that juxtaposes sandstone bedrock and overlying units 2 and 3 on the west with a distal alluvial fan deposit on the east (Figure 10). The fault strikes N25ºW across the trench and dips sub vertically. Here, the fault extends upward through warped distal alluvial fan deposits into the modern soil, and is expressed as an approximately 1.25-m-wide zone of high- and low-angle fracturing (Figure 10). A steepening of eastward tilted bedding with increasing depth across the zone of warping and faulting indicates recurrent deformation through time (Figure 10). This fault strand also coincides with a groundwater barrier (seep) and vegetation lineament.

Similar to trench T-1, a low-angle, west-dipping fault is exposed at the western end of trench T-3 between stations 7 and 10. The fault strikes N89ºW and dips 37ºSW across the trench, and is characterized by a thin (3-4 mm thick), grey clay gouge lining the fault plane at the base of the trench. Fault striae preserved in the clay gouge indicate oblique-slip displacement consistent with reverse–dextral slip. Vertical offset of alluvial fan deposits (units 2 and 3) west of the main active trace provides evidence for up-to-the-west vertical deformation (Figure 10), consistent with the fault striae. The vertical displacement appears to have back-tilted units 2, 3, 5, 6, and 7 west of the fault (Figure 10).

Trench T-3 provides evidence of aseismic creep along the Green Valley fault zone. About 2 m east of the main fault strand is a zone of subvertical open fractures that extend from the base of the trench to the ground surface. We observed similar open fractures along the creeping trace of the San Andreas fault in Bitterwater Valley (Cashman et al., 2003). We infer that the open fractures exposed in trench T-3 may also be related to fault creep. The fractures are oriented between N0ºW and N10ºW, which is more northerly than the strike of the fault zone. We interpret these fractures, and the apparent clockwise rotation of the fractures upsection, as Reidel shears accommodating some of the present-day dextral aseismic creep of the Green Valley fault. Based on the juxtaposition of different geologic units on either side of the fault near the base of the trench, warped alluvial fan deposits across the fault in the upper portion of the trench, and open extensive, subvertical fractures, we infer that the main trace of the Green Valley fault is exposed in trench T-3.

In summary, between trenches T-1 and T-3, the main active trace of the Green Valley fault is relatively well constrained based on geomorphology, and exposures in the trenches. The main active zone of deformation is characterized by a component of west-side up vertical displacement and a relatively narrow (<3 m wide) zone of fracturing that is likely associated with aseismic creep. Between the exposures in trenches T-1 and T-3, and the change in gradient of Lopes Ranch Creek across the fault zone, the southern segment of the Green Valley fault is constrained at the site as an approximately N25º-30ºW-striking fault zone and is clearly expressed based on a vegetation lineament and an east-facing scarp.

3.3 Displaced Paleo-Lopes Creek Channel Deposits

Paleochannels identified southeast of the GVF in trenches T-1 and T-4 include (1) a fluvial channel deposit having prominent channel morphology and an erosional basal contact (unit 7A), and (2) an overlying series of nested, thin, lenticular fluvial channel deposits (unit 9A). We infer that the unit 7A paleochannel deposit represents the abandoned channel of paleo-Lopes Ranch Creek, and therefore, this buried paleochannel can be used as a strain gauge to assess slip rate of the Green Valley fault. Units 7A and 9A are within the middle fluvial sequence and contain poorly sorted, subangular to subrounded clasts of siltstone and sandstone derived from the west. Both fluvial channel deposits are laterally continuous between trenches T-1 and T-4 for a distance of about 8 m (Figure 6). The unit 7A paleochannel trends N16ºE in trench T-1 and bends to a more northerly trend (N5ºW to N13ºW) in trench T-4. The paleochannel deposit is approximately 2 m wide and 0.75 m thick (Figures 6, 7, 9 and 13). On the basis of thalweg orientation and an absence of channels of similar appearance in trench T-2, the channel likely projects northeast of the eastern limit of trench T-2 (Figure 6). Based on clast lithologies that indicate a western source, channel dimensions, and a thalweg orientation that is similar to present-day Lopes Ranch Creek, as well as a slight northerly plunge (~3º).

Unit 9A paleochannel deposits range in thickness from about 10 to 25 cm and are up to 4 m wide (Figures 7 and 9). The northeastern and southwestern margins of these deposits roughly parallel the trend of unit 7A, suggesting the existence of a former valley aligned with the paleo-drainage of unit 7A (Figure 6). Although these deposits have channel morphology, and contain fine gravel of sandstone and siltstone lithology, also indicating a western source, they are not as deeply incised as unit 7A, and may represent a change in the depositional regime within the former Lopes Ranch Creek stream valley from incision to aggradation. This change in depositional regime may reflect changes in channel geometry (i.e. channel elongation, gradient shallowing) due to offset of the Lopes Ranch Creek channel along the GVF. Because of the absence of a clear channel thalweg associated with unit 9A, we favor using the clear thalweg of unit 7A to estimate total displacement of paleo-Lopes Creek across the Green Valley fault.

As shown on Figure 6, the southeastern limit of the exposed channel deposits are about 28 m where observed in trench T-1 from Lopes Ranch Creek. In our limited exploration, we did not observe a piercing point where the paleochannel deposits of unit 7A are in contact with the fault. We tentatively consider two end members that capture the uncertainty in the location of unit 7A at the fault zone. This first end-member model projects the trend of the unit 7A paleochannel deposits southwest from trench T-1 to the fault along an alignment that is parallel to the trend of the present day Lopes Ranch Creek. This model shows the minimum offset of 31 m across the fault (Figure 6). The second end-member model assumes that the paleochannel deposit projects southwest along the trend measured in trench T-1 (S16ºW), the paleochannel deposit of unit 7A may intersect the fault at about 58 m from the mouth of Lopes Ranch Creek (Figure 6). This larger displacement likely represents the near-maximum displacement of the paleochannel deposit.

3.4 Creep Rate Assessment

In an effort to assess the historic surface creep rate of the southern GVF, we originally planned to reoccupy and survey two existing USGS quadrilateral monuments across the fault in the vicinity of the Lopes Ranch Creek site. We planned to compare new surveyed offset measurements to previously measured offsets (Sims, J. USGS personal communication; 1998) to determine the width of the fault zone over which active creep is occurring and to document the fault creep rate over the last ten years. Unfortunately, we were unable to locate the monuments at Lopes Ranch. Instead, we documented creep on the GVF based on measuring the offset of a rock wall near Cordelia in a collaborative investigation with the U.S. Bureau of Reclamation (Figure 2).

In collaboration with Larry Anderson of the U.S. Bureau of Reclamation, we assisted in the survey of a pre-1862 rock wall that intersects the Green Valley fault to assess the width of the creeping fault zone and historical creep rate of the fault. Speculation on the offset of the rock wall was first presented by Frizzel and Brown (1976) as being offset across the Green Valley fault. The wall crosses at least two mapped strands of the Green Valley fault north of Interstate 80 and directly southwest of the Reservoir Lane site (Baldwin and Lienkaemper, 1999) (Figure 2). Preliminary survey results provide direct evidence for aseismic creep across one strand (central), and possibly a second strand (western) of the Green Valley Fault (Larry Anderson, 2004 personal communication). Across the central fault strand, the survey indicates that the rock wall is right-laterally offset between 0.2 and 0.5 m, with possible reverse drag (Figure 14). In addition, it is permissible to interpret as much as 0.5 m of dextral displacement of the rock wall across the western strand, although this is less definitive than measurements of slip on the central strand. Uncertainty associated with the western strand stems from the wall's location within a deep swale. At the swale, it appears that the wall may be undergoing downslope creep that could result in apparent right-lateral displacement. In addition, 1 km south-southeast of the site near the Intersection of I-80 and Highway 12, Borchardt (2001) encountered undeformed early to middle Holocene stratigraphy across the mapped location of the western fault strand suggesting that this strand is not active to the northwest, and that slip may be transferred to the easternmost fault strands (i.e., central and eastern fault strands at the rock wall site) (Figure 2). Alternatively, on the basis of the Borchardt (2001) trench locations, it is possible that the western fault strand projects between two trenches and thus went undetected.

L. Anderson currently is evaluating these preliminary estimates of displacement. Between the western and central fault strands, the preliminary results of the survey suggest a poorly constrained creep rate ranging from 1.4 to 7 mm/yr over a 142 year interval. Assuming that only the central fault strand is creeping, the creep rate may be refined to 1.4 to 3.5 mm/yr. Clearly, the age of the rock wall needs to be refined, if possible, to provide a better estimate of the aseismic creep rates.

4.0 DISCUSSION

The primary goal of this investigation of the southern GVF at the Lopes Ranch Creek site is to provide information on the fault's Holocene geologic slip rate. Because of the absence of clearly definable microstratigraphy and an absence of charcoal in many of the alluvial deposits at the site, deciphering earthquake timing information was not possible. Current earthquake probability models for the San Francisco Bay area consider slip rate estimates for the GVF derived from creep studies (Galehouse, 1998; Galehouse and Lienkaemper, 2003) and trench studies (Borchardt et al., 1999; Baldwin and Lienkaemper, 1999; Borchardt and Baldwin, 2001) and estimate a slip rate of 5±3 mm/yr (WGCEP, 2003). Our investigation at the Lopes Ranch Creek site provides supplementary information to help confirm and refine the existing body of knowledge for the GVF.

4.1 Tectonic Model for Paleochannel Offset at Lopes Ranch Creek

Laterally offset streams and paleochannels have been used by various workers to evaluate slip rate and earthquake history of Holocene active faults such as the San Andreas fault in southern California (Wallace, 1968a; Sieh, 1978b; Sieh and Jahns, 1984; Grant and Sieh, 1993, 1994), the San Andreas fault in northern California (Fumal et al., 2003), and the Calaveras fault (Kelson et al., 1997; Baldwin et al., 2002). In a tectonic setting characterized by strike-slip faulting, ephemeral streams are usually diverted laterally along the fault zone and are unlikely to reoccupy their former channel after every coseismic surface-fault displacement (McCalpin, 1996). Wallace (1990) described the process in which a stream channel adjusts to progressive strike slip offset by elongation and channel gradient shallowing. This causes alluvial deposition in the stream channel and eventually causes the stream to spill across the fault trace and create a new channel more in alignment with the channel upstream from the fault (Sieh and Jahns, 1984; Wallace, 1990).

We propose two alternative tectonic models to explain the paleochannel offset observed at the Lopes Ranch Creek site (Figure 15). The first model, the progressively offset channel model, assumes that right lateral offset along the GVF deflects the channel to the southeast because alluvial fan material, originally present north of the creek, is translated along the fault, partially blocking the stream valley along its northern margin (Figure 15B). Although the stream may follow the new deflected course for a short period of time, the alluvial fan material on the northern margin of the stream valley likely is eroded rapidly, allowing the stream to reoccupy its previous position (Figure 15C). The deflected channel is then abandoned. Colluvial and slack-water fluvial deposits then fill in the abandoned stream valley. The process of channel offset followed by abandonment is repeated after each earthquake, or each couple of earthquakes. This process would result in multiple abandoned channel deposits preserved southeast of the creek (Figure 15D).

The second model, the elongated channel model, assumes that the channel is deflected to the southeast due to right lateral offset along the fault, similar to the progressively offset channel model (Figure 15F). In this model, the stream is unable to erode quickly the alluvial fan material that partially blocks the creek valley, forcing the creek to flow along the deflected channel. Each time the creek is right laterally offset either by coseismic displacement or aseismic creep, the stream channel is lengthened and its gradient is shallowed (Figure 15G). This causes the stream to deposit sediment in the elongated reach, which begins to fill up the stream valley. It is only after sufficient aggradation has occurred that the stream can overtop its banks, abandon the deflected reach, and incise a new channel in the stream's original position (Figure 15H). The abandoned channel and stream valley that contains it would then be filled by alluvial fan sediments and colluvium. The stratigraphic record of this process would be preserved southeast of the creek as a single channel deposit overlain by fine-grained fluvial deposits and migrating channel deposits.

On-going fault creep would translate the abandoned stream valley deposits farther to the southeast. The process would repeat after another large earthquake.

Depending on the magnitude of offset along the fault during a surface rupturing earthquake, it is possible that the stream may adjust to the offset in a manner similar to either of the proposed offset models described above. However, based on trench exposures, the elongated channel model is more consistent with the stratigraphic relations observed at the Lopes Ranch Creek site for several reasons. First, the deepest channel deposit (unit 7A) has the most prominent channel morphology and is similar in orientation and size to the modern Lopes Ranch Creek channel. Second, fluvial deposits that bury the thalweg channel are characterized by overbank sandy silt with discontinuous nested channels (unit 9A). The lack of deep incision at the base of unit 9A channel deposits suggests that the stream was migrating across the stream valley and aggrading. The stratigraphic package containing units 7A, 9, and 9A, and the lack of other channel deposits implies that the Lopes Ranch Creek channel was filled by fluvial deposits and then abandoned. Additionally, the stratigraphic evidence does not support multiple channel abandoning events. The alluvial fan and colluvial deposits that subsequently buried the fluvial deposits indicate an abrupt end to fluvial deposition. We infer that fluvial deposits ceased to accumulate in the Lopes Ranch stream valley because a sufficient depth of aggradation had occurred allowing the stream to flood its banks and erode a new channel more in line with the thalweg west of the fault. Continued creep and/or surface fault rupture has transported the abandoned channel deposits to the south to their present location.

4.2 Preliminary Slip Rate of the Green Valley Fault

At this time, available subsurface information is insufficient to assess whether the progressively offset channel or elongated channel models is most applicable to the Lopes Ranch Creek site. Regardless, preliminary estimates of paleochannel displacement (unit 7A) incorporate the uncertainties of both models and indicate dextral offset ranging between 31 and 58 m (Figure 6). Based on the preferred age of unit 8 (14,080 to 15,380 cal yr B.P.), which postdates unit 7A, a maximum slip rate estimate ranges from 2 to 4 mm/yr. The range in slip rate reflects a 95% confidence based on assumed models of paleo-channel geometry (Figure 6). We consider the rate a maximum for the fault strands crossing the site, and because of a younger overlying unit used to estimate the minimum age of unit 7A. We acknowledge that this study is preliminary and the findings should be considered initial. Clearly additional trenching is necessary to delineate the southwest projection of unit 7A into the fault zone, and to assess the presence or absence of multiple offset paleochannel deposits to test the hypothesized displacement models for the site. Multiple offset paleochannel deposits may provide data for paleo earthquake timing and coseismic displacement.

4.3 Conclusions

We excavated one trench across the GVF northwest of Lopes Ranch Creek. Southeast of the creek, we excavated two trenches across the center of a linear swale and one trench across the GVF and swale. The trenches exposed a broad fault zone possibly up to 12 m wide that contains vertical faults, west-dipping dextral-reverse oblique faults, and fractures indicative of fault creep. The trenches exposed Green Valley sequence bedrock and overlying massive fine-grained alluvial and fluvial deposits consisting of clayey silt to sandy silt. The stratigraphic relations exposed in the trenches are not conducive for the recognition and preservation of event timing stratigraphy. However, the trenches did encounter a prominent paleochannel deposit with a clear channel thalweg overlain by a series of nested lenticular channel deposits. We interpret these paleochannel deposits to represent the southeastern extension of the former Lopes Ranch Creek channel. We also infer that channel lengthening and gradient shallowing led to aggradation within the stream valley that eventually caused the channel to abandon its deflected course and establish its present-day incised channel.

The Lopes Ranch creek site, which lies along the southern GVF, is characterized by a late Pleistocene creep rate (~2-4 mm/yr), prominent tectonic geomorphology, and a southeast trending linear swale within which late Holocene sediments have accumulated. The presence of buried stream-channel deposits southeast of the present-day stream channel provides the opportunity to estimate a preliminary latest Pleistocene-Holocene slip rate of the southern GVF. The paleochannel deposits have a mapped minimum dextral offset of about 31 m, and are possibly offset up to 58 m. The minimum age of the channel deposits – 14,080 to 15,380 yr B.P. –is based on a radiocarbon sample collected from a soil and burn layer developed in a fine-grained overbank deposit that overlies unit 7A. Based on the poorly constrained offset and minimum age of the offset channel, we estimate a late Pleistocene slip rate for the southern GVF of about 2 to 4 mm/yr. This slip rate estimate is consistent with a slip rate previously determined at Lopes Ranch over a 300-yr-time span for the GVF and at Galindo Creek for the Concord fault (Borchardt et al., 1999). The late Pleistocene creep rate is close to the modern aseismic creep rate of 4.4 ± 0.1 mm/yr measured at Red Top Road near Cordelia (Galehouse and Lienkaemper, 2003). Lastly, it overlaps with the preferred slip rate of the main creeping strand of the Green Valley fault near Cordelia as determined from a survey of an approximately 142 yr old rock wall offset across the fault.

In summary, the Lopes Ranch Creek site provides an initial long-term geologic slip rate for the southern Green Valley fault. The stratigraphic and structural relations encountered during this initial study suggest that this site provides an excellent opportunity to determine the geologic slip rate for the Green Valley fault. Additional subsurface studies are recommended to: (1) refine the age of unit 7A, (2) better characterize the cumulative displacement of unit 7A, and (3) assess the geometric relations of unit 7A directly at the fault zone.

5.0 REFERENCES

Anderson, L., 2004, personal communication.

Baldwin, J.N., and Lienkaemper, J.J., 1999, Paleoseismic investigations along the Green Valley, Solano County, California: Unpublished Report - Bay Area Paleoseismological Experiment Contract No: 98WRCN1012, 18 p.

Baldwin, J.N., Kelson, K.I., Witter, R.C., Koehler, R.D., Helms, J.G., and Barron, A.D., 2002, Preliminary report on the late Holocene slip rate along the central Calaveras Fault, southern San Francisco Bay Area, Gilroy, California: Final Technical Report, U.S. Geological Survey, National Earthquake Hazards Reduction Program, 27 p.

Baldwin, J.N., and Koehler, R.D., 2002, Paleoseismic Feasibility Study of the Green Valley Fault, San Francisco Bay Area, California: Final Technical Report, U.S. Geological Survey, Award 01-HQ-GR-0123, p. 1-25.

Baldwin, J.N., Unruh, J.R., and Lettis, W.R., 1998, Neotectonic investigation of the northward extension of the Green Valley fault, Napa County, California: Final Technical Report to the U.S. Geological Survey National Earthquake Hazards Reduction Program, 2 plates, 27 p.

Baldwin, J.N., Unruh, J.R., and Lettis, W.R., 1998, Neotectonic map of lineaments, folds and faults in the Howell Mountains Napa Valley region, California: Final Technical Report, U.S. Geological Survey, Award 1434-HQ-96-GR-02738, scale 1:24,000.

Borchardt, G.S., 2003, personal communication.

Borchardt, G.S., David L; Wills, Chris J., 1999, Holocene slip rate of the Concord Fault at Galindo Creek in Concord, California: National Earthquake Hazards Program Final Technical Report, National Earthquake Hazards Program, U.S. Geological Survey, Library, Reston, VA, United States.

Borchardt, G.S., 2000, Holocene slip rate of the Green Valley fault at Freeborn Creek, Fairfield, California: National Earthquake Hazards Program Final Technical Report, National Earthquake Hazards Program, U.S. Geological Survey, Library, Reston, VA, United States. Award No. 98HQGR1039.

Borchardt, G.S., and Baldwin, J.N., 2001, Late Holocene behavior and seismogenic potential of the Concord-Green Valley fault system in Contra Costa and Solano Counties, CA, *in* Ferriz, H., and Anderson, R., eds., Engineering Geologic Practice in Northern California: California Division of Mines and Geology, Bulletin 210, Special Publication 12, p. 229-238.

Bryant, W.A., 1992, unpublished Fault Evaluation Report FER-232, Southern Green Valley fault, Solano County: California Division of Mines and Geology, map scale 1:24,000, 14 p.

Bryant, W.A., 1991, The Green Valley fault, *in* Figuers, S. (Chairman), Field trip guide to the geology of western Solano County: Northern California Geological Society, Association of Engineering Geologists, and Rogers/Pacific, p. 1-11.

Bryant, W.A., 1982, Green Valley fault zone, Cordelia and Mt. George quadrangles, California: California Division of Mines and Geology, Unpublished Fault Evaluation Report FER-126, map scale 1:24,000.

Carey, D.S., 1991, The Green Valley fault zone, between Marsh View Road and Highway 80, Cordelia, California *in*, Field trip guide to the Geology of Western Solano County, October 12, 1991, Northern California Geological Society Association of Engineering Geologists, and Rogers/Pacific, Inc., p. 17-24.

Cashman, S.M, Baldwin, J.N., and Cashman, K.V., 2003, Investigation of microscale fault textures associated with aseismic creep and coseismic rupture in active fault zones [abs.]: Eos (Transactions, American Geophysical Union), 2003 Fall Meeting, San Francisco, CA, December 8-12, 2003.

Cashman, S.M., Baldwin, J.N., Cashman, K.V., 2003, Investigation of microscale fault textures associated with aseismic creep and coseismic rupture in active fault zones [abs.]: Proceedings of the Hayward fault workshop, eastern San Francisco Bay area, California, September 19-20, 2003, p. 6.

Crane, R., 1988, Unpublished Geologic Map of the Cordelia 7.5 minute Quadrangle, California.

Ellsworth, W.L., Olson, J.A., Shijo, L.N., and Marks, M., 1982, Seismicity and active faults in the eastern San Francisco Bay region, *in* Hart, E.M., Hirschfeld, S.E., and Schulz, S.S., Proceedings-Conference on earthquake hazards in the eastern San Francisco Bay area: California Division of Mines and Geology Special Publication 62, p. 83-91.

Fox, K.F., Jr., 1983, Tectonic Setting of Late-Miocene, Pliocene and Pleistocene Rocks in part of the Coast Ranges North of San Francisco, California: U.S. Geological Survey Professional Paper 1239, 33p.

Frizzell, V.A., Jr., and Brown, R.D., Jr., 1976, Map showing recently active breaks along the Green Valley fault, Napa and Solano Counties, California: U.S. Geological Survey Miscellaneous Field Studies Map MF-743, scale 1:24,000.

Fumal, T.E., Heingartner, G.F., Dawson, T.E., Flowers, R., Hamilton, J.C., Kessler, J., Reidy, L.M., Samrad, L., Seitz, GG., Southon, J., 2003, Recurrence Interval for the San Andreas Fault, Southern San Francisco Bay Area, California [abs.]: American Geophysical Union, Fall meeting, December 8-12, San Francisco, Abstracts and Program, p.129.

Galehouse, J.S., 1998, Theodolite measurements of creep rates on San Francisco Bay region faults [abs.]: U.S. Geological Survey NEHRP Web Page (http://erp-web.er.usgs.gov/reports/abstract/1998/nc/g3111fin.htm), 6 p.

Galehouse, J.S., and Lienkaemper, J.J., 2003, Inferences drawn from tow decades of alinement array measurements of creep on faults in the San Francisco Bay region: Bulletin of the Seismological Society of America, v. 93, no. 6, p. 2415-2433.

Grant, L.B., and Sieh, K.E., 1993, Stratigraphic evidence for seven meters of dextral slip on the San Andreas fault during the 1857 earthquake in the Carizzo Plain: Bulletin Seismological Society of America, v. 83, p. 619-635.

Grant, L.B., and Sieh, K.E., 1994, Paleoseismic evidence of clustered earthquakes on the San Andreas fault in the Carizzo Plain, California: Journal of Geophysical Research, v. 99, p. 6819-6841.

Kelson, K.I., Baldwin, J.M., and Randolph, C.E., 1997, Geologic slip rate along the southern Calaveras fault at San Ysidro Creek, near Gilroy, California: American Geophysical Union, v. 78, no. 76, p. F439.

Kelson, K.I., Lettis, W.R., and Lisowski, M., 1992, Distribution of geologic slip and creep along faults in the San Francisco Bay region, *in* Borchardt, G., Hirschfeld, S.E., Lienkaemper, J.J., McClellan, Patrick, Williams, P.L., and Wong, I.G., eds., Proceedings of the Second Conference on Earthquake Hazards in the Eastern San Francisco Bay Area: California Department of Conservation, Division of Mines and Geology Special Publication 113, p. 31-38.

Kelson, K.I., Simpson, G.D., Lettis, W.R., and Haraden, C., 1996, Holocene slip rate and earthquake recurrence of the northern Calaveras fault at Leyden Creek, northern California: Journal of Geophysical Research, v. 101, no. B3, p. 5,961-5,975.

Lienkaemper, J.J., and Borchardt, G., 1996, Holocene slip rate of the Hayward fault at Union City, California: Journal of Geophysical Research, v. 101, no. B3, p. 6099-6108.

McCalpin, J.P. (ed.), 1996, Paleoseismology, Volume 62, Chapter 2, International Geophysics Series, Academic Press.

Niemi, T.M., and Hall, N.T., 1992, Late Holocene slip rate and recurrence of great earthquakes on the San Andreas fault in northern California: Geology, v. 20, no. 3, p. 195-198.

Oppenheimer, D.H., and Macgregor-Scott, N., 1992, The seismotectonics of the eastern San Francisco Bay region, *in* Borchardt, G., Hirschfeld, S.E., Lienkaemper, J.J., McClellan, Patrick, Williams, P.L., and Wong, I.G., eds., Proceedings of the Second Conference on Earthquake Hazards in the Eastern San Francisco Bay Area: California Department of Conservation, Division of Mines and Geology Special Publication 113, p. 11-16.

Petersen, M.D., Bryant, W.A., Cramer, C.H., Cao, T., Reichle, M.S., Frankel, A.D., Lienkaemper, J.J., McCrory, P.A., and Schwartz, D.P., 1996, Probabilistic seismic hazard assessment for the state of California; California Department of Conservation, Division of Mines and Geology, Open file Report 96-08, 33p.

Prentice, C.S., 1989, Earthquake geology of the northern San Andreas Fault near Point Arena, California: California Institute of Technology, Pasadena, Ph.D. thesis, 246 p.

Sawyer T.L. and Unruh, J.R., 2002, Paleoseismic investigation of the Holocene slip rate on the Greenville fault, eastern San Francisco Bay area, California: Final Technical Report, National Earthquake hazards Reduction Program Award 00-HQ-GR-0055.

Schwartz, D.P., Pantosti, D., Hecker, S., Okumura, K., Budding, K.E., and Powers, T., 1992, Late Holocene behavior and seismogenic potential of the Rodgers Creek fault zone, Sonoma County, California, *in* Borchardt, G., Hirschfeld, S.E., Lienkaemper, J.J., McClellan, Patrick, Williams, P.L., and Wong, I.G., eds., Proceedings of the Second Conference on Earthquake Hazards in the Eastern San Francisco Bay Area: California Department of Conservation, Division of Mines and Geology Special Publication 113, p. 393-398.

Sieh, K.E., 1978b, Slip along the San Andreas fault associated with the great 1857 earthquake: Bulletin Seismological Society of America, v. 68, p. 1421-1448.

Sieh, K.E., and Jahns, R.H., 1984, Lateral offsets and revised dates of large prehistoric earthquakes at Pallett Creek, southern California: Journal of Geophysical Research, v. 89, p. 7641- 7670.

Simpson, G.D., Baldwin, J.N., Kelson, K.I., Lettis, W.R., 1999, Late Holocene slip rate and earthquake history for the northern Calaveras fault at Welch Creek, eastern San Francisco Bay area, California: Bulletin of Seismological Society of America, v. 89, p. 1250-1263.

Simpson, G.D., Lettis, W.R., and Kelson, K.I., 1992, Segmentation model for the Northern Calaveras fault, Calaveras Reservoir to Walnut Creek, *in* Borchardt, G., Hirschfeld, S.E., Lienkaemper, J.J., McClellan, Patrick, Williams, P.L., and Wong, I.G., eds., Proceedings of the Second Conference on Earthquake Hazards in the Eastern San Francisco Bay Area: California Department of Conservation, Division of Mines and Geology Special Publication 113, p. 253-259.

Sims, J.D., 1998, personal communication.

Sims, J.D., 1993, Parkfield area tectonic framework [abs.]: *in* Jacobson, M.L., ed., Summaries of technical reports, Volume XXXIV Prepared by participants in the National Earthquake Hazards Reduction Program: U.S. Geological Survey Open-File Report 93-195, p. 682-684.

Unruh, J.R., 1999, personal communication.

Unruh, J.R., and Lettis, W.R., 1999, Kinematics of transpressional deformation in the eastern San Francisco Bay region, California: Geology, v. 26, no. 1, p. 19-22.

Unruh, J.R., and Sawyer, T.L., 1997, Assessment of blind seismogenic sources, Livermore Valley, eastern San Francisco Bay Region: Final Technical Report for NEHRP Award No. 1434-95-G-2611, p. 95.

Wagner, D.L., and Bortugno, E.J., 1982, Geologic Map of the Santa Rosa Quadrangle, California: California Division of Mines and Geology, Regional Geologic Map Series, Santa Rosa quadrangle, Map 2A (Geology), Sheet 1 of 5, scale 1:250,000.

Wallace, R.E., 1968a, Notes on stream channels offset by the San Andreas fault, southern Coast Ranges, California, *in* Dickinson, W.R. and Grantz, A., eds., Geological Problems of the San Andreas Fault System, Stanford University Publication Geological Sciences 11, p. 6-21.

Wallace, R.E., ed., 1990, The San Andreas fault system, California: U.S. Geological Survey Professional Paper 1515, 283 p.

Working Group on California Earthquake Probabilities, 1999, Earthquake probabilities in the San Francisco Bay Region: 2000 to 2030 – a summary of findings: U.S. Geological Survey Open-file Report 99-517, 60 p.

Working Group on California Earthquake Probabilities, 2003, Earthquake Probabilities in the San Francisco Bay region: 2002-2031: U.S. Geological Survey Open-File Report 03-214

Working Group on Northern California Earthquake Potential, 1996, Database of potential sources for earthquakes larger than magnitude 6 in northern California: U.S. Geological Survey Open-file Report 96-705, 53 p.

FIGURES

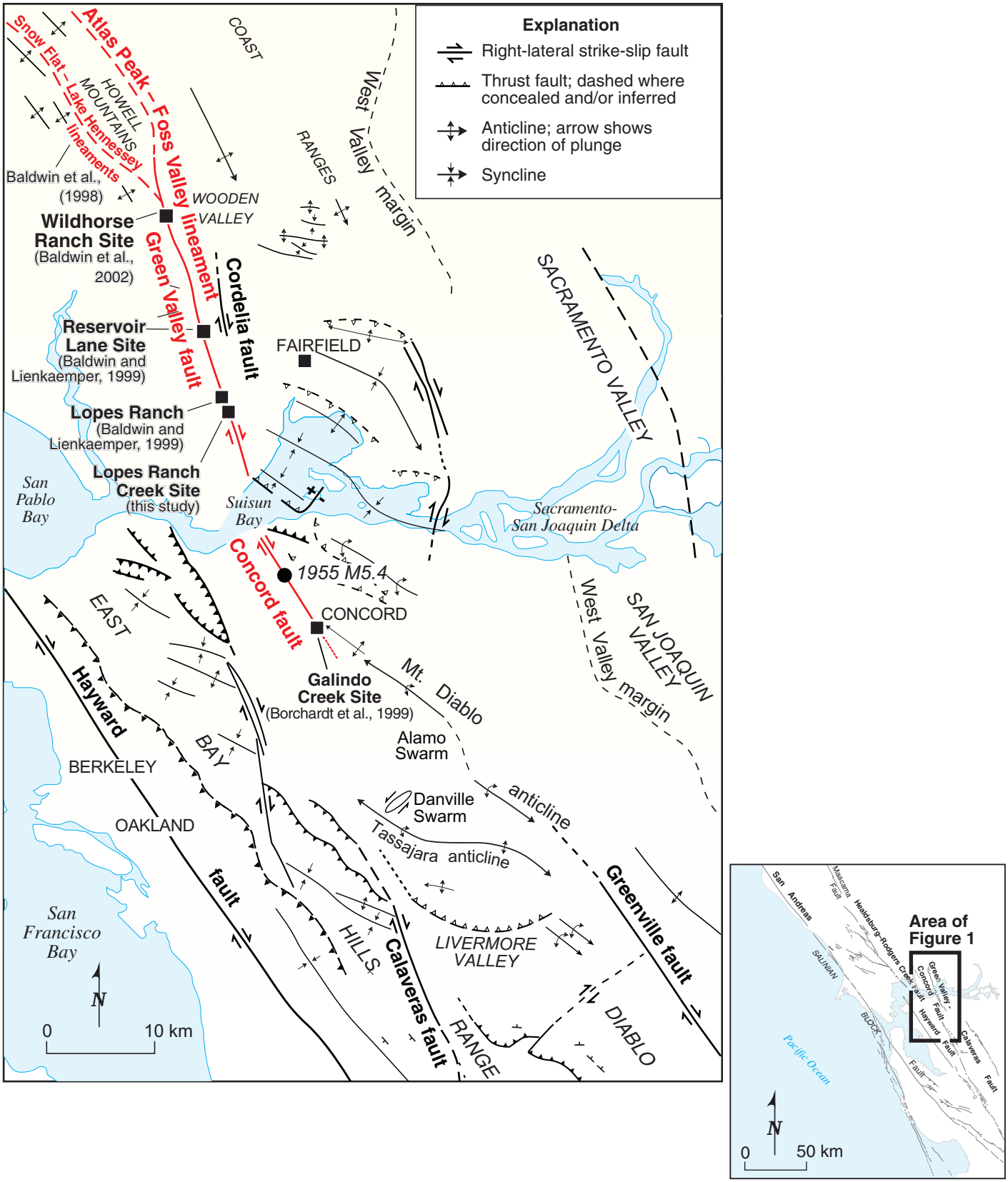

Figure 1. Concord-Green Valley fault system, and other faults in the eastern San Francisco Bay area.

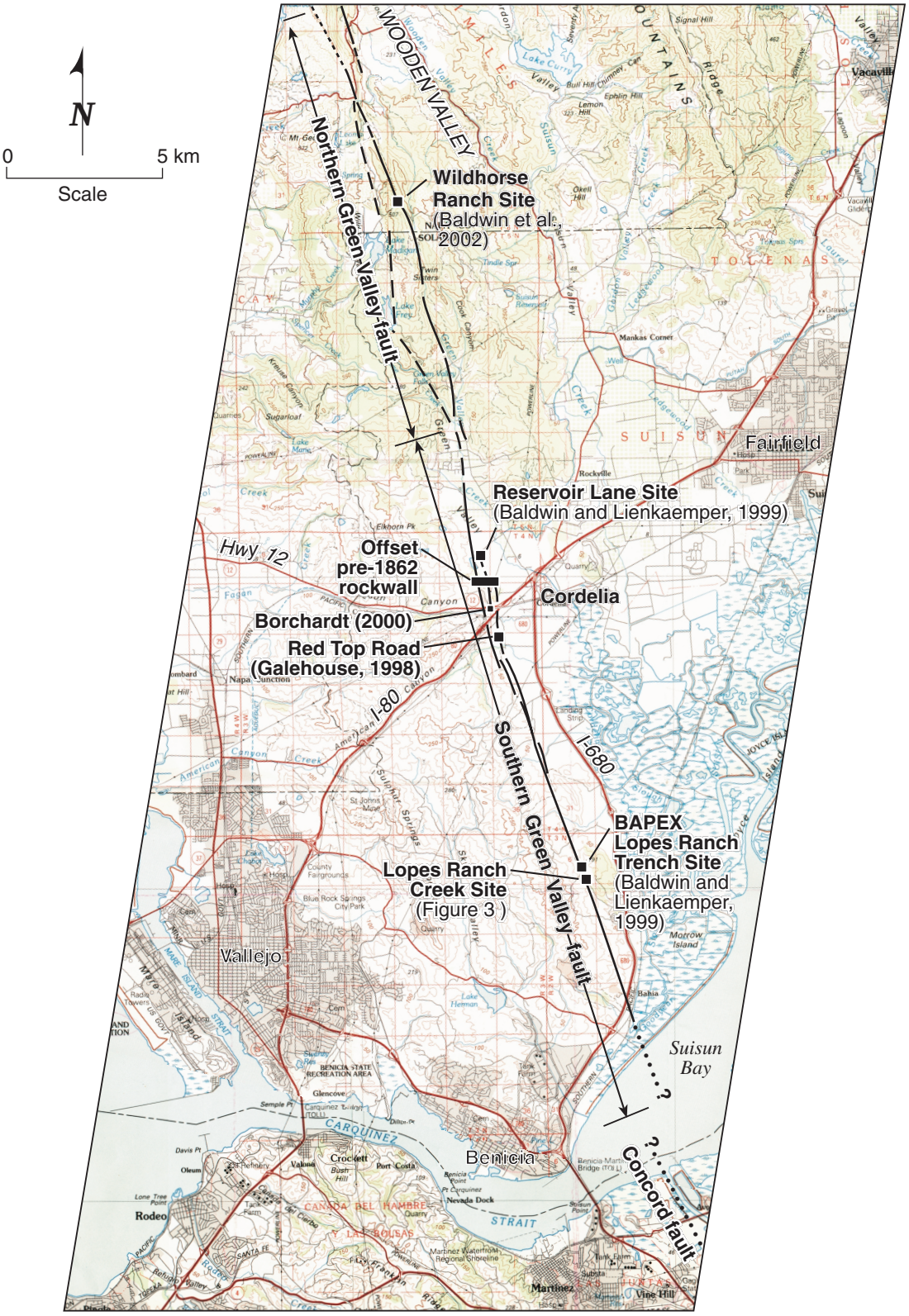

Figure 2. Fault location map showing location of previous paleoseismic and geoarchaeological studies on the Green Valley fault (modified from Bryant, 1982; and Baldwin et al., 1998).

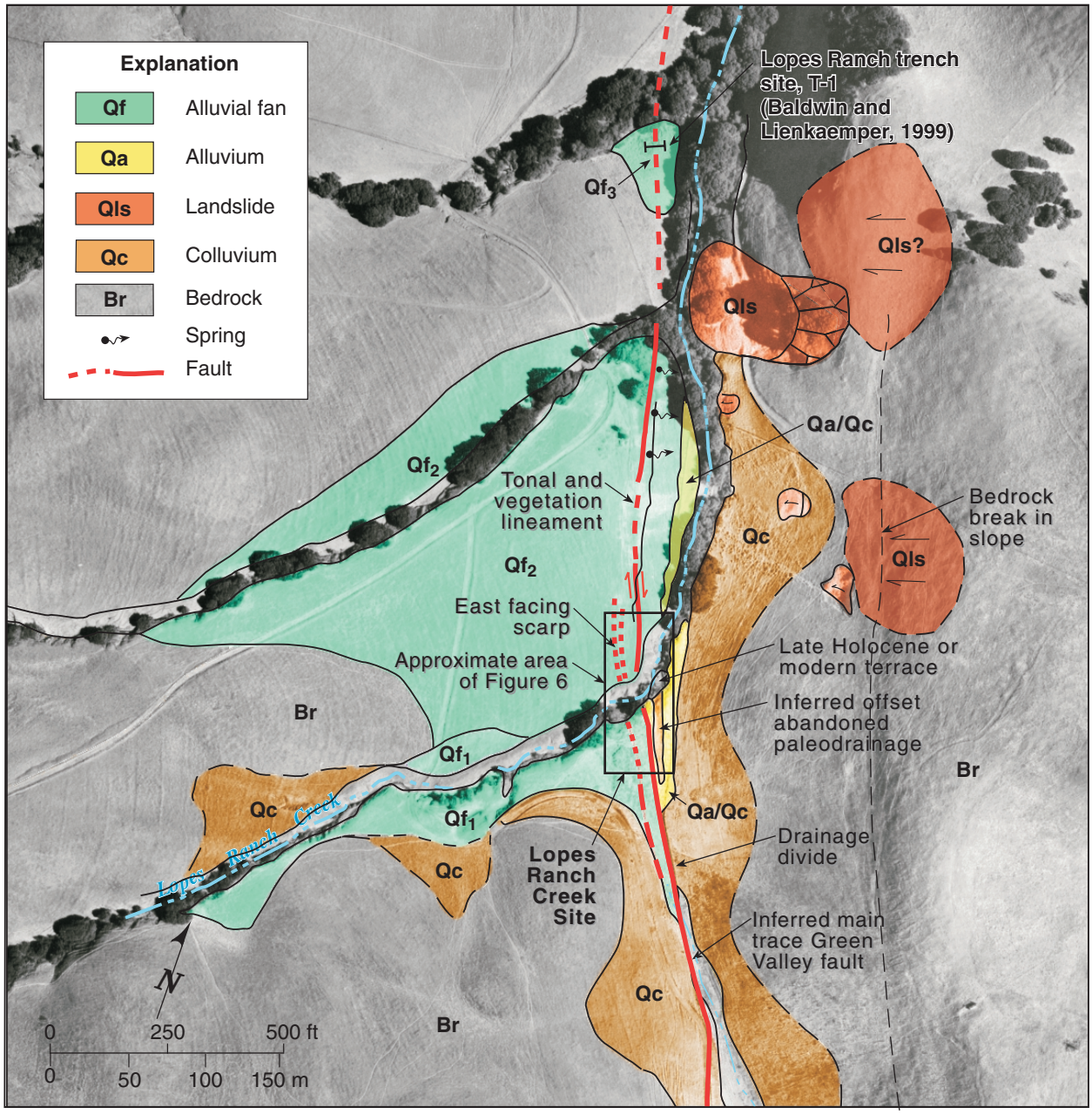

Figure 3. Aerial photograph interpretation of the Southern Green Valley fault at the Lopes Ranch Creek Site and Quaternary geologic map units and fault traces. Photograph from 1996.

Figure 4. Photograph looking southeast showing linear saddle and fault valley extending southeast of the Lopes Ranch Creek site. Mount Diablo and Suisun Bay are in the background.

Figure 5. Photograph looking northwest showing broad alluvial fan incised by Lopes Ranch Creek (trending across middle ground). Lopes Ranch Creek bends to the north at the Green Valley fault and follows a linear stream valley to the northwest.

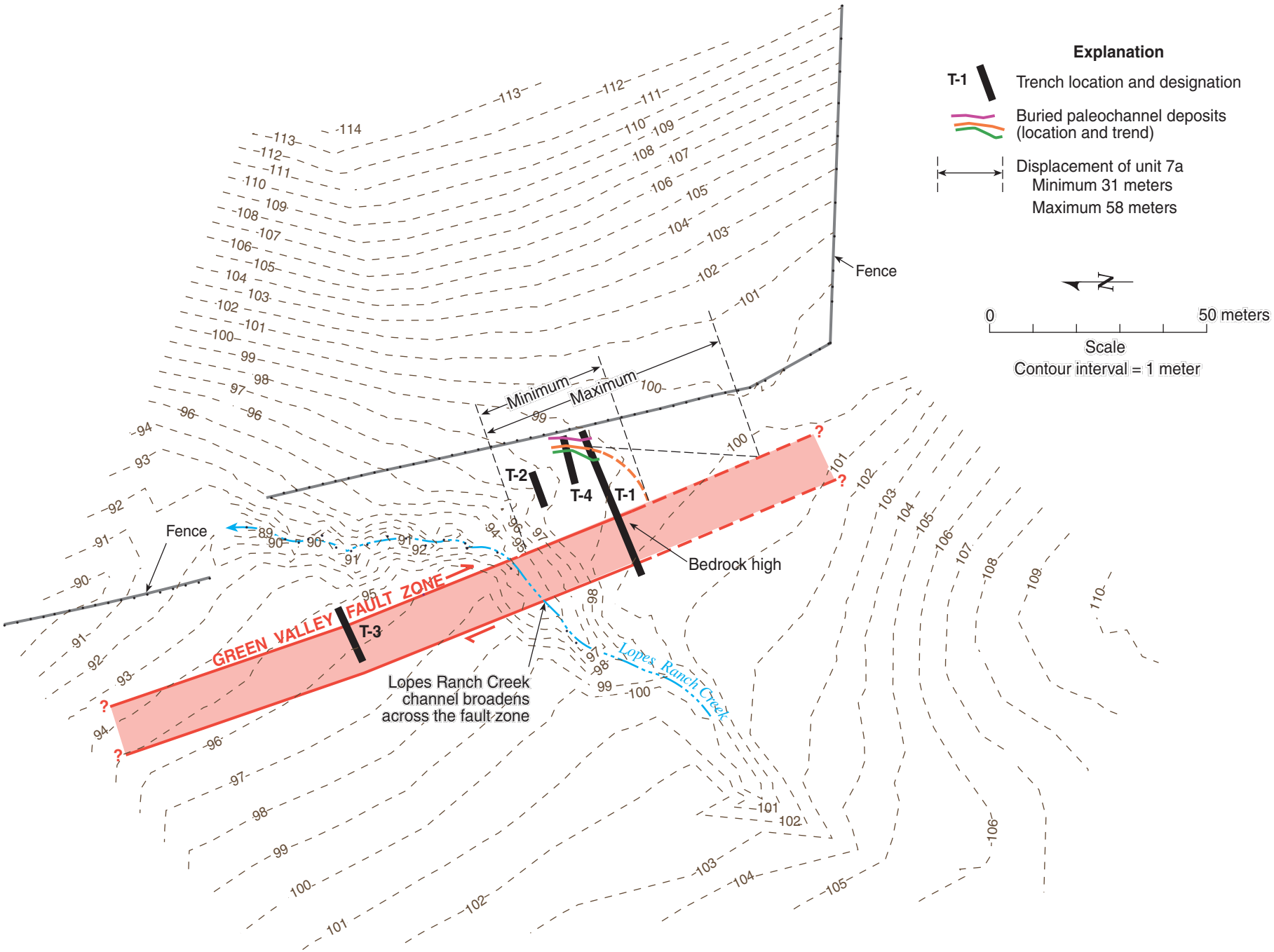

Figure 6. Detailed topographic map of the Lopes Ranch Creek site. Green and purple lines through trenches T-1 and T-4 represent the western and eastern limit of buried channel deposits. Orange line represents the thalweg of the deepest channel deposit (unit 7A). The minimum and maximum displacements of unit 7A are also shown.

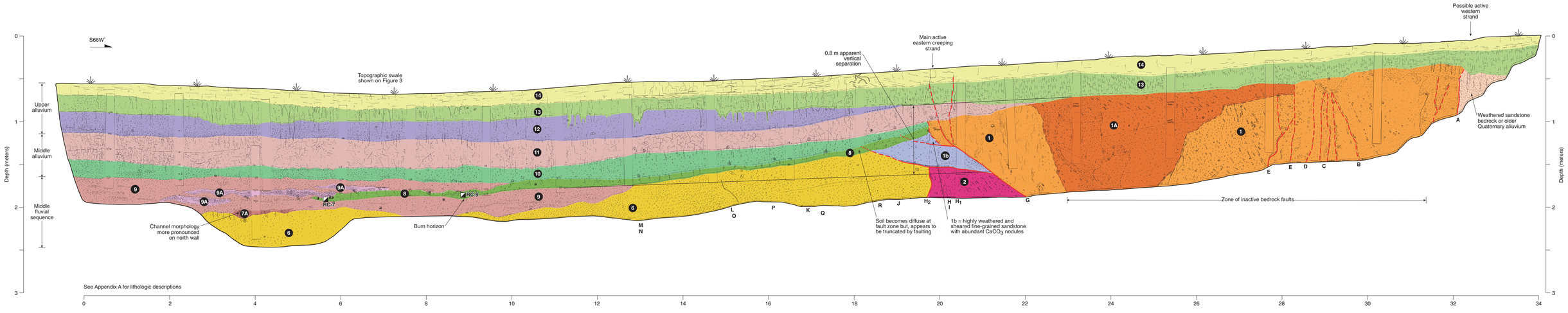

Explanation

S66˚W˚ — Trench orientation

Fault, dashed where approximate; arrow shows direction of movement

RC-7 — Radiocarbon sample location and designation (see Table 1)

Fault Orientations

- **A** N18˚W, 90˚ ($CaCO_3$ along fault)
- **B** N18˚W, 78˚SW
- **C** N28˚W, 90˚
- **D** N27˚W, 90˚
- **E** N23˚W, 90˚
- **F** N23˚W, 90˚; N28W, 90˚
- **G** N50˚W, N30˚W, N20˚W, N33˚W, 26˚
- **H** N15˚E, 5˚W (upper low angle fault straie suggest reverse dextral shear. On north wall offsets Unit 11)
- **H_1** N - S±5, 8˚W±2 (straie 70˚ from south; reverse dextral shear on lower low angle fault)
- **H_2** N30˚W, 90˚

Bedding Attitudes for Unit 11

- **I** N39˚W, 15˚NE
- **J** N29˚W, 12˚NE
- **K** N55˚W, 12˚NE
- **L** N40˚W, 3˚NE
- **M** N62˚W, 0˚

Bedding Attitudes for Unit 10

- **N** N38˚W, 4˚NE
- **O** N15˚W, 7˚NE
- **P** N9˚W, 13˚NE
- **Q** N11˚W, 16˚NE
- **R** N62˚W, 0˚

Note: Locations of attitudes designated by letters are shown below log.

L O P E S R A N C H

Trench T-1
South Wall

WLA William Lettis & Associates, Inc. | Figure 7

1575 Lopes Ranch

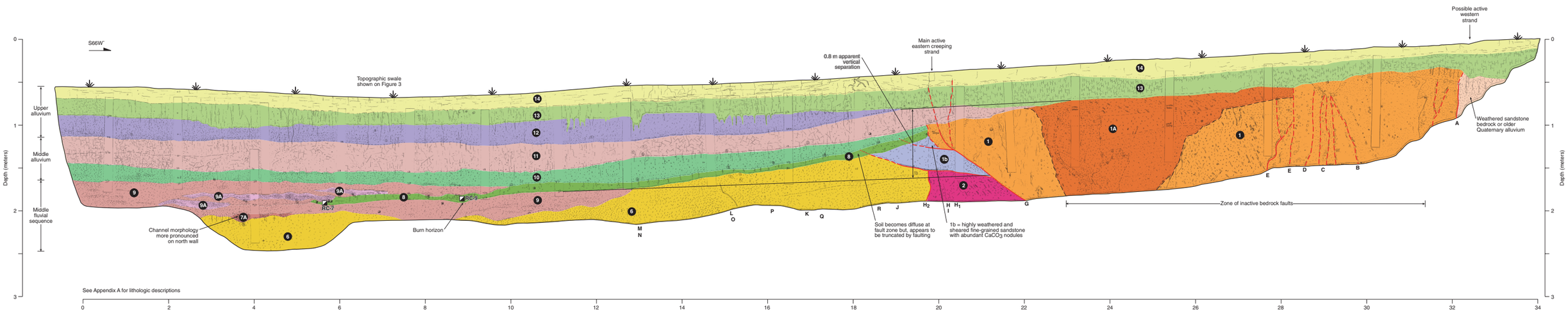

Explanation

S66°W — Trench orientation

Fault, dashed where approximate; arrow shows direction of movement

RC-7 — Radiocarbon sample location and designation (see Table 1)

Fault Orientations

- **A** N18°W, 90° ($CaCO_3$ along fault)
- **B** N18°W, 78°SW
- **C** N28°W, 90°
- **D** N27°W, 90°
- **E** N23°W, 90°
- **F** N23°W, 90°; N28W, 90°
- **G** N50°W, N30°W, N20°W, N33°W, 26°
- **H** N15°E, 5°W (upper low angle fault straie suggest reverse dextral shear. On north wall offsets Unit 11)
- **H_1** N - S±5, 8°W±2 (straie 70° from south; reverse dextral shear on lower low angle fault)
- **H_2** N30°W, 90°

Bedding Attitudes for Unit 11

- **I** N39°W, 15°NE
- **J** N29°W, 12°NE
- **K** N55°W, 12°NE
- **L** N40°W, 3°NE
- **M** N62°W, 0°

Bedding Attitudes for Unit 10

- **N** N38°W, 4°NE
- **O** N15°W, 7°NE
- **P** N9°W, 13°NE
- **Q** N11°W, 16°NE
- **R** N62°W, 0°

Note: Locations of attitudes designated by letters are shown below log.

L O P E S R A N C H

Trench T-1
South Wall

WLA William Lettis & Associates, Inc. | Figure 7

1575 Lopes Ranch

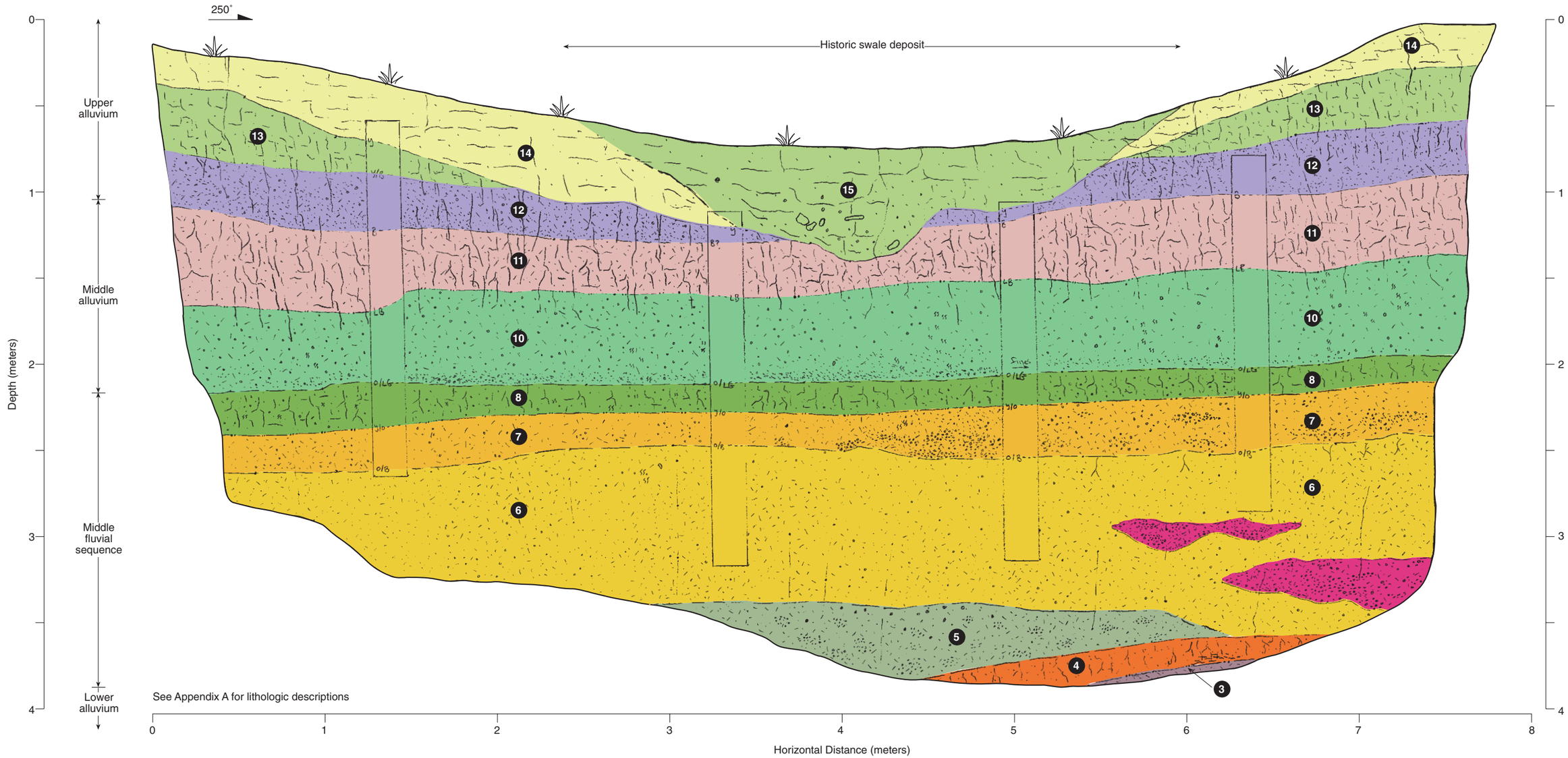

Explanation

250° Trench orientation

LOPES RANCH	
Trench T-2 **South Wall**	
WLA William Lettis & Associates, Inc.	Figure 8

1575 Lopes Ranch

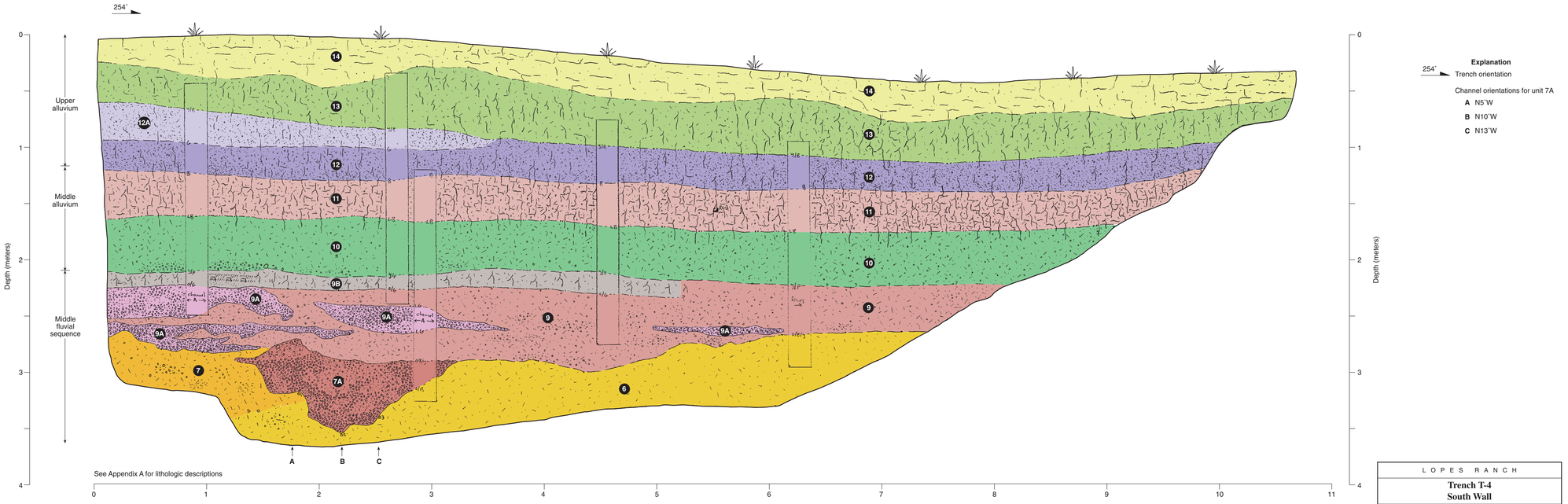

LOPES RANCH

Trench T-4
South Wall

WLA William Lettis & Associates, Inc. | Figure 9

1575 Lopes Ranch

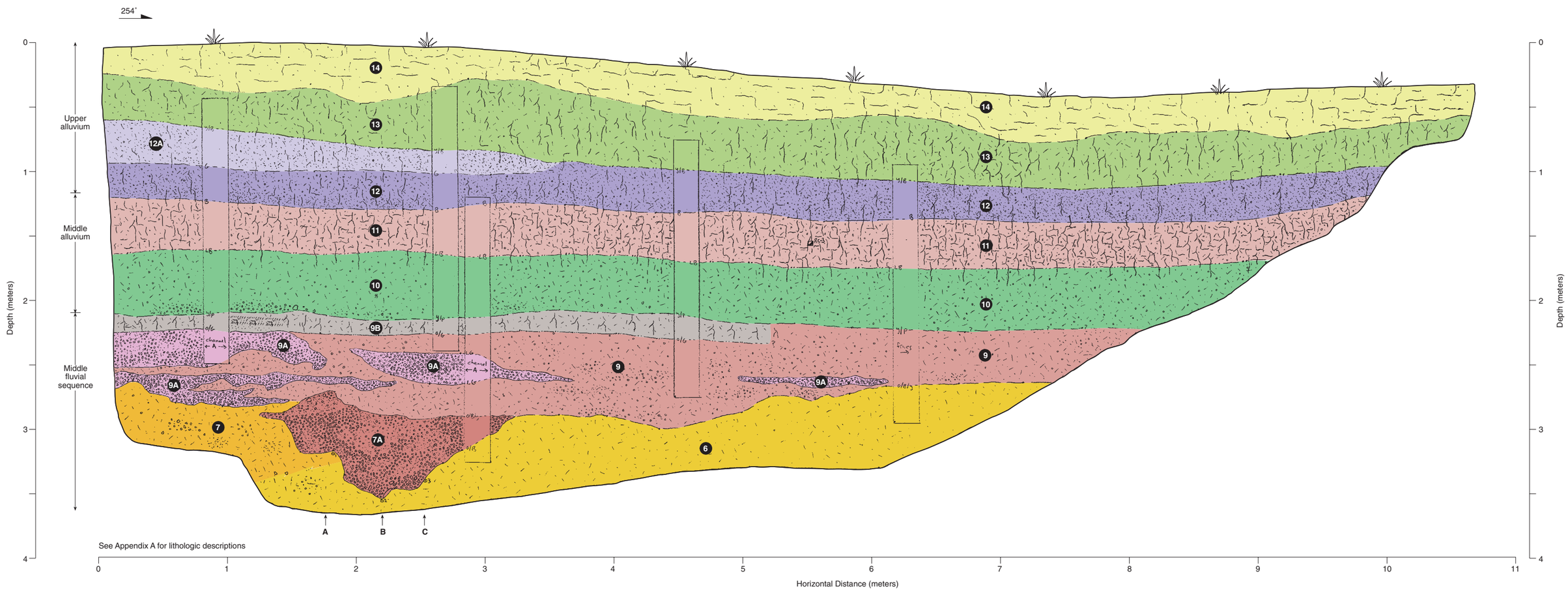

Explanation

254° Trench orientation

Channel orientations for unit 7A

A N5°W

B N10°W

C N13°W

L O P E S R A N C H

Trench T-4
South Wall

WLA William Lettis & Associates, Inc. | Figure 9

1575 Lopes Ranch

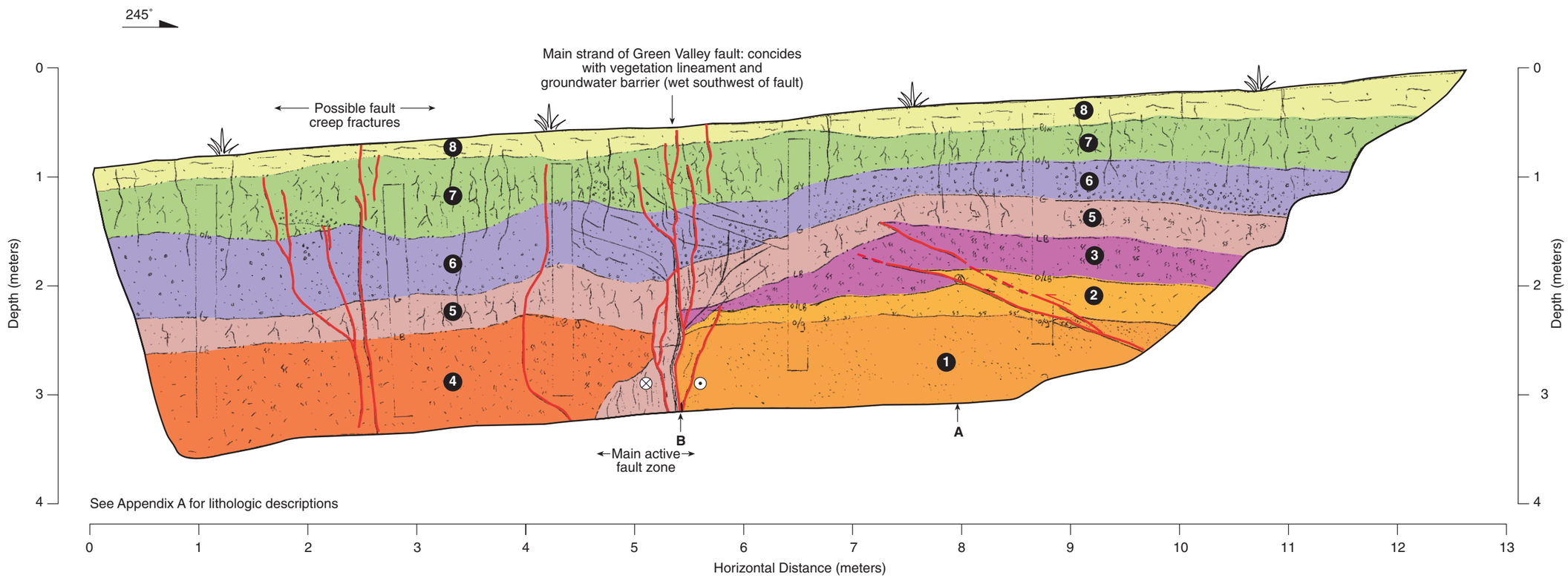

Explanation

245° Trench orientation

Fault, dashed where approximate; arrow shows direction of movement

Fault Orientations

A N89°W, 37°SW

B N25°W, vertical

LOPES RANCH	
Trench T-3 **South Wall**	
WLA William Lettis & Associates, Inc.	Figure 10

1575 Lopes Ranch

A)

B)

Figure 11. Photographs of Green Valley fault zone in trench T-1 showing altered sandstone bedrock. (A) shows altered sandstone bedrock in fault contact with darker brown alluvium. (B) shows older shear planes being replaced by calcium carbonate in sandstone bedrock.

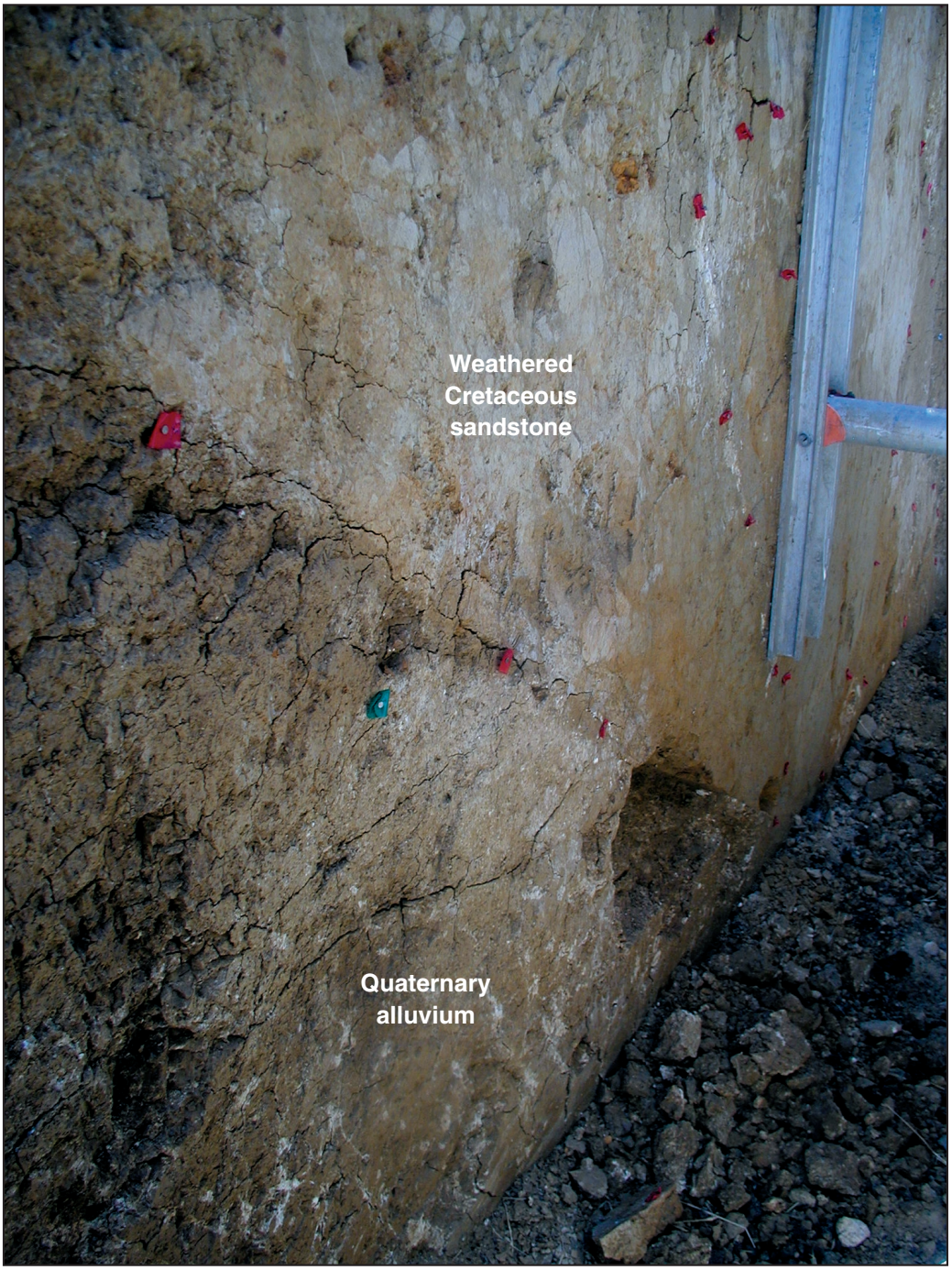

Figure 12. Low-angle fault juxtaposing weathered bedrock on the west over Quaternary alluvial fan deposits on the east in the south wall of trench T-1. Photograph corresponds with Station 22m.

Figure 13. Photograph of south wall of trench T-4 showing paleochannel unit 7A overlain by thinner paleochannels of unit 9.

A)

B)

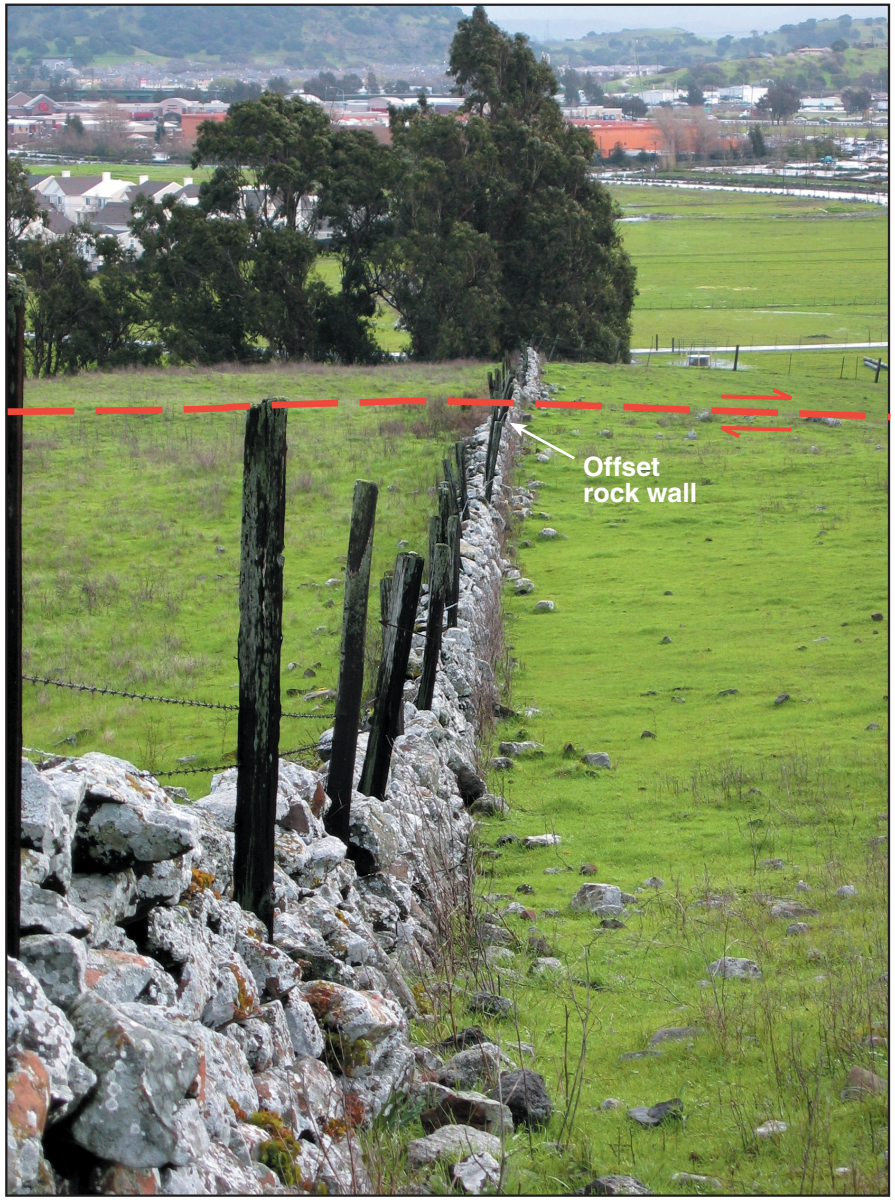

Figure 14. (A) View to west shows rock wall crossing central fault strand of the Green Valley fault and showing displacement. (B) View to the east showing right-laterally deflected rock wall across the central fault strand of the Green Valley fault.

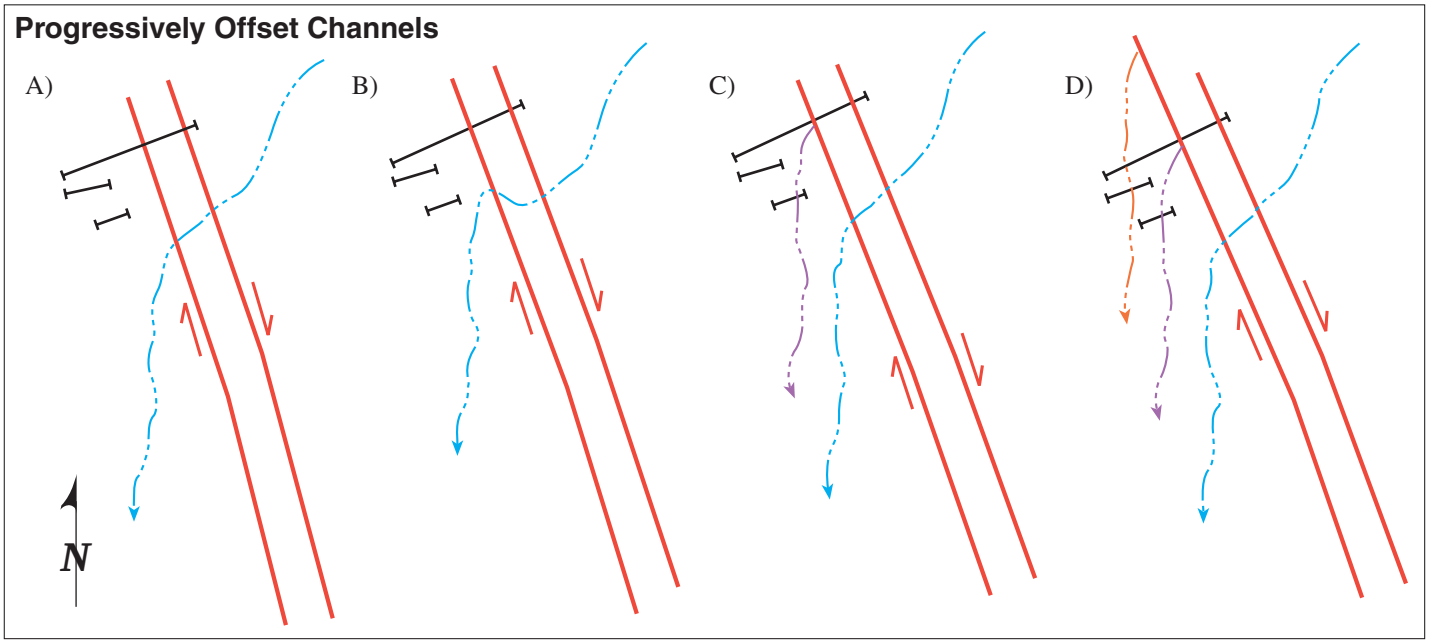

A) Stream flows across fault

B) Stream offset by fault creep/rupture

C) Stream rapidly returns to original stream channel and only flows in elongated segment for a short time. Stream rapidly erodes material transported across the stream channel along the fault

D) Process repeates over multiple earthquake cycles leaving a stratigraphic record of multiple discreet channel deposits

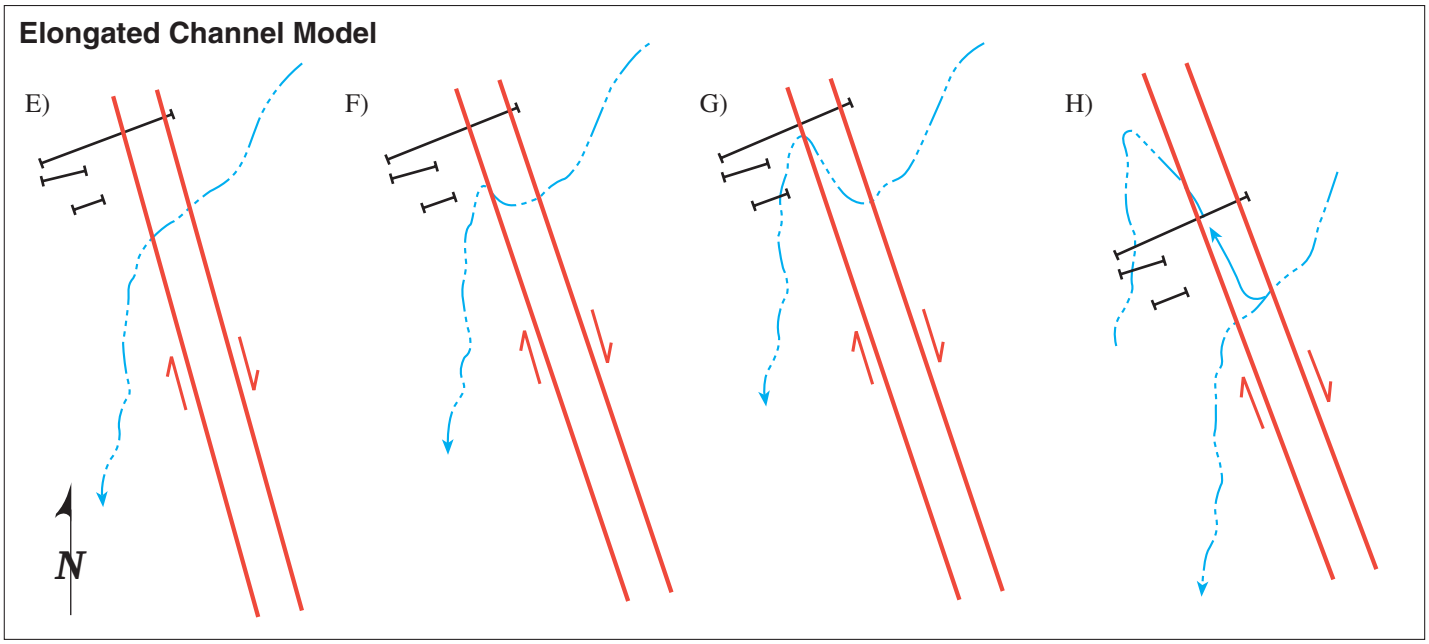

E) Stream flows across fault

F) Stream offset by fault creep/rupture

G) Continued offset elongates channel and shallows gradient causing aggradation in stream valley

H) Further offset and ongoing aggradation fills stream valley. High discharge event causes stream to overtop its banks and incise new channel more in line with original channel.

Figure 15. Two alternative models to explain the observed buried paleochannel deposits at Lopes Ranch Creek.

APPENDIX A -

LITHOLOGIC AND PEDOLOGIC DESCRIPTIONS

Lopes Ranch Creek Trenches T-1, T-2, and T-4

Unit 15 - Silt (ML), 10YR 3/1 very dark gray, approx. 15% clay, subangular blocky peds (1-2 cm), non-sticky, slightly plastic, massive, many vf. roots, many f. and vf. pores, contains large subangular to sub-rounded clasts up to 6 cm. long, contains horseshoe and nails (Historic swale colluvium).

Unit 14 - Silt (ML) with trace gravel, 2.5Y 3/1 (m) very dark gray, massive, 95% fines with about 20% as clay, and <5 % coarse, gravels average between 1-2 mm diameter, subangular, many fine and very fine pores, no clay films present, pedogenic structure is subangular blocky (1-2 cm), also contains granular blocky peds 3 mm to 0.5 cm that are not present in unit below. (Holocene colluvium with A-horizon soil development)

Unit 13 - Clayey silt (ML) with trace gravel, 2.5 Y 3/1 (m) very dark gray, 20% clay, <5% coarse-grained fraction (less than unit below), massive, peds are subangular blocky (2-3 cm), many fine to very fine pores, very weak clay films, peds are extremely hard, slightly sticky and plastic, unit is overprinted by the modern A/B soil horizon, gradational basal contact (Holocene colluvium)

Unit 12 - Sandy silt (ML) to clayey silt (ML) with trace gravel, 2.5 Y 3/2 (m) very dark grayish brown, >55% fines, clay content ranges from approx. 15% in sandy silt zones to 25-30% in clayey silt zones, <15% coarse-grained fraction, massive, mottled orange and gray, fine-grained sand visible on ped faces, nonsticky, slightly plastic, many fine and very fine pores, peds are firm, angular blocky (1-3 cm), weak to no clay films, coarse-grained fraction of deposit consists of weathered, glassy Sonoma volcanics (derived from east), gradational wavy to smooth basal contact (Holocene Colluvium or distal alluvial fan deposit).

Unit 11 - Silty clay (CL) to clay (CL) with sand and gravel, 2.5 Y 3/2 (m) very dark grayish brown, 90% fines with approx. 30-35% clay, 10% coarse-grained fraction, mottled orange and gray, gravel consists of sandstone and volcanic clasts are sub-rounded to sub-angular, up to 1 cm diameter, with average at about 2-3 mm, massive, slight increase in coarseness with depth, peds are very firm to extremely firm, coarse angular blocky (3-5 cm) with medium clay films on ped faces, sticky, plastic, many fine to very fine pores, contains trace fine carbonate nodules <0.5 cm diameter, gradational wavy to smooth basal contact, unit represents buried Bt horizon (Holocene Colluvium or distal alluvial fan deposit).

Unit 10 - Sandy to Silty clay (CL) with trace gravel, 2.5Y 4/3 to 4/4 (m) olive brown, >95% fines with 35-40% clay, <5% coarse-grained, gravel clasts consist of sub-angular to sub-rounded volcanic and sandstone fragments up to 0.5 cm diameter with average between 1-2 mm, massive, contains occasional discontinuous fine pebble lenses or laminations, pedologic structure is firm, angular blocky (1-3 cm) with thick clay films on ped faces, contains ~10% fine carbonate nodules <0.5 cm diameter with occasional nodules up to 3 cm diameter, clear to gradational and wavy to smooth basal contact (Distal alluvial fan/colluvium with soil development).

Unit 9B - Clayey silt (ML) with trace gravel, 2.5Y 4/4 (m) olive brown, 90% fines and 10% coarse-grained fraction, generally massive but contains faint thin laminations of clay (dark brown) with sand (yellowish-brown), contains primarily sandstone clasts derived from the west and a trace of volcanic clasts derived from east, pedogenic structure medium angular blocky (1-3 cm) with thick clay films on pedogenic fractures, peds are firm to slightly friable, unit extends across the eastern end of trench T-4 and becomes very diffuse to absent to southwest, occurs at

a similar stratigraphic level as unit 8 in trench T-1, soil is less developed and is probably slightly younger than unit 8, soil most likely not developed in western side of trench T-4 due to active fluvial processes at time of development, (Holocene buried soil horizon developed in fluvial overbank deposit).

Unit 9 - Clayey silt (ML) with trace fine sand, yellowish brown, mottled yellow brown to dark olive brown, approximately 20-30% clay, contains <10% pea gravel randomly distributed throughout, >90% fine, diffuse to gradual basal contact, unit eroded through and onlaps unit 8, contains discontinuous, lenticular, interfingering channel deposits (shown as unit 9A on log), channels consist of 30-60% pea gravel averaging 1 cm and up to 10 cm long, subangular to subrounded, thin clay coatings on clasts, poorly sorted, no bedding, clasts are primarily tan sandstone and siltstone, no volcanic clasts suggesting a western source, grain supported where gravel content >40% and matrix supported where gravel content <40%, matrix is sandy silt, orientation of unit 9A channels ranges from N10W to N35ºW and dip <3 degrees NW (late Pleistocene-to Holocene alluvial/fluvial overbank deposit).

Unit 8 - Clayey silt (ML) to silty clay (CL), dark yellowish brown to dark olive brown, contains < 5-10% fine grained sand and <1 cm diameter clasts of sandstone, siltstone and chert, massive, trace very fine carbonate nodules in laminations, weak clay films on ped faces, peds are angular blocky (1-3 cm), firm, the eastern 6 meters of unit is slightly darker where charcoal is present, unit rises to west up scarp, carbonate content increases towards scarp, unit was eroded by unit 9 at the western end of trench T-1 (late Pleistocene buried soil horizon developed in fluvial overbank deposits).

Unit 7 - Clayey silt (ML), 2.5Y 4/4 (m) olive brown, mottled orange and brown with dark brown root haloes, massive, approx. 30% clay, >90% fine, <10% coarse, massive with subtle gravel stringers, gravels up to 0.5 cm, average 1-2 mm, thin clay films on ped faces, very few very fine pores, basal contact clear over 3 cm, slightly coarser than unit 6, contains prominent channel deposit (shown as unit 7A on log) that is massive to weakly bedded, 10YR 4/4 dark yellowish brown, gravel clasts are greenish mudstone and red, tan, and purple sandstone and siltstone suggesting a western source, subangular to subrounded clasts in the 1-3 cm range and abundant 1-5 mm clasts, channel orientation in trench T-4 are N5ºW (east channel margin), N13ºW (west channel margin), N10ºW (channel thalweg), channel orientation in trench T-1 is N16ºE, some zones are matrix supported with grain supported pockets, channel has irregular erosional basal contact, (late Pleistocene fluvial overbank and channel deposit).

Unit 6 - Clay (CL) olive brown 2.5Y 4/4 mottled orange brown, >95% fines with approximately 40% clay, <5% coarse-grained fraction, contains clasts of mudstone and sandstone up to 0.5 cm with average at about 1-2 mm diameter, sticky, plastic, no pores and no roots, to the north in trench T-2 unit becomes clayey silt (ML) with trace sand and gravel, contains two discontinuous channel deposits that have about 75% fines and 25% sand and gravel, gravel up to 0.5 cm and average 2 mm, subrounded, (Holocene fluvial overbank deposit).

Unit 5 - Silt (ML) with trace sand and gravel, 2.5Y 4/4 (m) olive brown, massive with discontinuous gravel lenses, about 85% fine and 15% sand and gravel, slightly sticky and plastic, gravel consists of subangular, red and tan mudstone and sandstone clasts averaging 1-3 mm and up to 1 cm, (Holocene alluvial to fluvial deposit).

Unit 4 - Silt (ML) with trace sand, 10YR 4/3 to 3/3 brown to dark brown, >95% fine and < 5% coarse, approx. 20% clay, slightly to non sticky, plastic, massive, contains charcoal, (Holocene buried soil developed in distal alluvial fan or fluvial overbank deposit).

Unit 3 - Silt (ML) with trace sand, 2.5Y 4/4 olive brown, mottled gray, >95% fine, <5% coarse, approx. 15% clay, slightly sticky, slightly plastic, massive, no bedding (distal alluvial fan or fluvial overbank deposit).

Unit 2 - Clayey silt (ML) with fine sand, dark yellowish brown, abundant carbonate coatings on fracture faces (Quaternary alluvium).

Unit 1A- Clayey fine-grained sand (weathered Cretaceous to Jurassic sandstone) with abundant carbonate coatings on fractures, and abundant nodules; contains occasional chert fragments; reddish to dark red yellowish brown.

Unit 1B- Clayey fine-grained sand (weathered Cretaceous to Jurassic sandstone) similar to unit 1A but with less calcium carbonate and an increase in clay content.

Unit 1 - Lower Cretaceous to Upper Jurassic Great Valley Sequence, marine sandstone, siltstone, mudstone, and conglomerate. Unit is only exposed in trench T-1, along eastern side of fault zone, rock is tan to slightly yellowish orange brown fine grained sandstone with well-developed anastomosing, dendritic fracture pattern that may be related to hydrothermal alteration of rock by fluids migrating through porous sandstone, in the western part of fault zone highly weathered sandstone clasts have been replaced with carbonate, many subvertical carbonate nodule stringers are oriented along subvertical fractures, more resistant blocks of sandstone (colored light orange on log) have had minor weathering from soil development processes, less resistant blocks (colored dark orange on log) have been highly weathered by soil development processes and contain large carbonate nodules up to 6 cm diameter, nodules have irregular form and have tubular centers.

Lopes Ranch Creek Trenches T-3

Unit 8 - Clayey silt (ML) to silty clay (CL), 10YR 3/1 very dark gray, trace granules and fine gravel soil structure is granular and has platy basal partings, massive, (AB horizon soil developed in colluvium or distal fan deposit)

Unit 7 - Clayey silt (ML) to silty clay (CL), 10YR 3/1 very dark gray, massive, hard to dense, gradual to diffuse basal contact, trace fine gravels, large columnar peds and occasional blocky peds, (B horizon soil developed in colluvium or distal alluvial fan deposit).

Unit 6 - Clayey silt (ML), 7.5YR 4/3 dark brown with strong brown overtones from weathered fine grained sandstone clasts, approx. 20-35% fine to med gravel, primarily matrix supported with clay films on ped faces, gravels typically <1 cm consisting of sandstone and dark olive brown siltstone, rare gravels up to several cm, fines up section, Soil fractures from unit 7 penetrate the top of unit and have dark brown stainings, unit fines to east with primarily fine granules in clay matrix, unit thickens over fault, basal contact is clear to gradual on western side of trench and becomes gradual to diffuse to east, (Alluvial fan deposit)

Unit 5 - Clayey silt (ML) to silty clay (CL) with trace gravel, 7.5YR 3/3 dark brown to 10YR 3/3 dark brown, approx 5-10% gravels, trace fine sand, slightly mottled with yellow brown blotches, hard to dense, massive with prismatic to blocky peds, approx. 10-15% carbonate nodules (typically <1 cm), carbonate occurs as stringers and random nodules, (Distal alluvial fan deposit).

Unit 4 - Clay (CL) to clayey silt (ML), 7.5YR 3/2 dark brown, massive, contains fine (<1 cm diameter) carbonate nodules, more carbonate than unit 5, likely correlates with unit 3, (Distal alluvial fan or fluvial deposit).

Unit 3 - Clayey silt (ML), 7.5YR 4/4 brown to 10YR 4/4 dark yellowish brown, massive approx. 30-40% carbonate nodules ranging from 1 to 5 cm long, very well developed, occasional MnO nodules, massive, mottled yellow brown to dark brown, hard, dense when dry, similar to unit 2 but slightly wetter, likely correlates with unit 4, (Distal alluvial fan deposit).

Unit 2 - Clayey silt (ML) with trace fine gravels, 10YR 6/4 light yellowish brown, light grayish brown when dry, massive, well developed prismatic to columnar peds, contains prominent 3-5 cm long carbonate nodules (more prominent in footwall of low angle fault (~20%$CaCO^3$), less carbonate upsection (5% $CaCO^3$), clear to gradual basal contact, (weathered bedrock or distal alluvial fan deposit).

Unit 1 - Lower Cretaceous to Upper Jurassic Great Valley Sequence, marine sandy siltstone to fine sandstone, 7.5YR 5/6 yellowish brown mottled with olive brown clay vienlets, contains pockets of fine granules, translocated clay from soil has made upper part of unit more clay rich, very friable (bedrock).